University of Salerno
Department of Chemistry and Biology

Ph.D Course in Chemistry
(XIII Cycle)

ENVIRONMENTAL AND CATALYTIC APPLICATIONS OF ALKALINE OXIDES

Supervisor
Prof. Antonio Proto

Ph.D Student
Raffaele Cucciniello

Co-Supervisor
Prof. Leone Oliva
Prof. Oriana Motta

Scientific referee
Prof. Vincenzo Venditto

Ph.D Course Coordinator
Prof. Gaetano Guerra

Academic year 2013-2014

Publications

- R.Cucciniello, A.Proto, D. Alfano, O. Motta. Synthesis, characterization and field evaluation of a new based-Ca CO_2 absorbent for radial diffusive sampler, *Athmospheric Environment* 60, (2012), 82-87

- R.Cucciniello, A.Proto, F. Rossi, O. Motta. Mayenite based supports for atmospheric NO_x sampling, *Athmospheric Environment* 79, (2013),666-671

- A.Proto, R.Cucciniello, F. Rossi, O. Motta. Stable carbon isotope ratio in atmospheric CO_2 collected by new diffusive device, *Environmental Science and Pollution Research*, 21 (4),(2014), 3182-3186

- A.Proto, R.Cucciniello, F. Rossi, O. Motta. Ca-based absorbents for NO_x measurements in atmospheric environments surrounding monumental and archeological sites, Procedings of conference Built Heritage 2013 – Monitoring conservation and management, pag.1447-1453, ISBN 978-88-908961-0-1

- O. Motta, R. Cucciniello, C. Scicali, A. Proto. A study on the applicability of zinc acetate impregnated silica substrate in the collection of hydrogen sulfide by active sampling, *Talanta*, 128, (2014), 268-272

- O. Motta, I. Zarrella, R. Cucciniello, G. Vigliotta, A. Proto. Study of the antibacterial activity in the gas phase of a chemical formulation for the household waste management, *Letters in Applied Microbiology*, accepted for publication

- A. Proto, R. Cucciniello, A. Genga, C. Capacchione. A study on the catalytic hydrogenation of aldehydes using mayenite as active support for palladium, *Catalysis Communications*, submitted 2014

Congress presentations

- A.Proto R.Cucciniello, C. Ardovino,O. Motta. The determination of atmospheric CO_2 by a passive sampling device. *Proceedings of Urban Environmental Pollution*, 14-17 june 2012, Amsterdam, The Netherlands

- R.Cucciniello, A.Proto, F. Rossi, O. Motta. Sviluppo di substrati inorganici a base di ossidi metallici per la determinazione simultanea di NO e NO_2 con campionatori passivi. *Proceedings of XIII Congresso Nazionale di Chimica dell'Ambiente e dei Beni Culturali,* 10-14 september 2012, Taranto, Italy

- O. Motta, F. De Caro, E. Santoro, L. Palmieri, C. Ardovino, G. Boccia, P. Cavallo, R.Cucciniello, A.Proto, M. Capunzo. Alternative al CS_2 per l'estrazione di BTEX da substrati a base di carbone attivo, *Proceedings of 45° Congresso Nazionale SITI*, 3-6 october 2012,Cagliari, Italy

- R.Cucciniello, A.Proto, F. Rossi, O. Motta. Nuovo substrato per il campionamento attivo di acido solfidrico in atmosfera, *Proceedings of XIV Congresso Nazionale di Chimica dell'Ambiente e dei Beni Culturali*, 2-5 june 2013, Rimini, Italy

- R.Cucciniello, F. Rossi, O. Motta, A.Proto. NO_x uptake on Ca-based absorbents", *Proceedings of International Conference on Chemistry and the Environment 2013*, 25-28 june 2013, Barcellona, Spain

- R.Cucciniello, C. Capacchione, O. Motta, A.Proto. Interaction between NO_x and Ca-based sorbents, *Proceedings of XLI Congresso di Chimica inorganica,* 3-6 september 2013, Parma, Italy

- R.Cucciniello, C. Capacchione, O. Motta, A.Proto. Catalytic aldehyde reduction in the presence of nanoporous calcium aluminate, *Proceedings of XLI Congresso di Chimica inorganica*, 3-6 september 2013, Parma, Italy

- A.Proto, R.Cucciniello, F. Rossi, O. Motta. Ca-based absorbents for NO_x measurements in atmospheric environments surrounding monumental and archeological sites, *Proceedings of Built heritage*, 18-20 november 2013, Milan, Italy

- R. Cucciniello, C. Pironti, C. Capacchione, O. Motta, M. Di Serio, A. Proto. Efficient conversion of glycidol to value-added products using heterogeneous catalysts, Proceedings of 5° Euchems Chemistry Congress, 31 August-4 September 2014, Istanbul (Turkey)

- R. Cucciniello, O. Motta, F. Esposito, F. Rossi, A. Proto. A new substrate for the active determination of hydrogen sulfide in air, Proceedings of 5° Euchems Chemistry Congress, 31 August-4 September 2014, Istanbul (Turkey)

- F. Rossi, A. Intiso, R. Cucciniello, O. Motta, N. Marchettini, A. Proto. A new technique for the determination of trichloroethylene diffusion matrix in water, *Proceedings of XXV Congresso della Società Chimica Italiana*, 7-12 September 2014, Rende, Italy

- R. Cucciniello, C. Pironti, C. Capacchione, M. Di Serio, A. Proto. Heterogeous catalysts for the production of glycols from glycerol derivates, *Proceedings of XXV Congresso della Società Chimica Italiana*, 7-12 September 2014, Rende, Italy

- R. Cucciniello, I. Zarrella, F. Rossi, O. Motta, A. Proto. Antibacterial chemical formulation for the household waste management, *Proceedings of XXV Congresso della*

Società Chimica Italiana, 7-12 September 2014, Rende, Italy

- R. Cucciniello, C. Pironti, C. Capacchione, M. Di Serio, A. Proto. Catalytic materials for the hydrogenation of glycidol to value-added products, *Proceedings of XXV Congresso della Società Chimica Italiana*, 7-12 September 2014, Rende, Italy

- R. Cucciniello, O. Motta, A. Proto. BTEX extraction from activated charcoal using dichloromethane as alternative to carbon disulfide, *Proceedings of the 1st VDI Expert Forum on Atmospheric Chemistry,* 19-20 November 2014, Bonn, Germany

Table of contents

Chapter III
Experimental part

Index of figures

Index of tables

List of abbreviations

IC: Ion chromatography
FT-IR: Infrared analysis using Fourier transform
TGA: Thermogravimetric analysis
XRD: X-ray diffraction
PM: Pure Mayenite ($Ca_{12}Al_{14}O_{33}$)
CM75: CaO/ $Ca_{12}Al_{14}O_{33}$ 75:25 wt%
CM35: CaO/ $Ca_{12}Al_{14}O_{33}$ 35:65 wt%
LOD: Limit of detection
NO_x: Nitrogen oxides
GC-FID: Gas chromatography with flame ionization detector
EO: Essential oils
MIC: Minimum inhibitory concentration
CFU: Colony forming unit
CO_2: Carbon dioxide
C12A7: $Ca_{12}Al_{14}O_{33}$; mayenite
C12A7:H: $Ca_{12}Al_{14}O_{33}$ doped with H^-
C12A7:e-: $Ca_{12}Al_{14}O_{33}$ doped with e^-
Ru: Ruthenium
HCl: Chloridric acid

Abstract

Alkaline oxides are widely used in industrial processes involving removal of gaseous compounds as unwanted by-products such as CO_2, hydrogen sulphide and nitric oxides. Traditional processes generally involve Ca-based sorbents for their high performances also at high-temperature, high availability, low costs and good recyclability in subsequent adsorption/desorption cycles.

Recently, interest about the use of new alkaline oxides in catalysis has increased considerably due to extraordinary discovery of an high active metal oxide namely mayenite, $Ca_{12}Al_{14}O_{33}$, able to take active part in catalytic reactions such as biomass steam reforming and nitrous oxide removal from the process gas of nitric acid plants.

Based on high reactivity of Ca-based sorbents towards gaseous acidic molecules, the first part of this thesis is dedicated to the employment of Ca-based sorbents in environmental devices, passive samplers, in order to evaluate their applicability as CO_2 and NO_x sorbents.

Moreover, the use of $Ca_{12}Al_{14}O_{33}$ as active support in catalysis is investigated in hydrogenation reactions comparing activity in terms of conversion and selectivity with those of commercial catalysts.

Introduction

The main aim of this thesis is to evaluate the applicability of Ca-based materials, particularly CaO and $Ca_{12}Al_{14}O_{33}$, as sorbents for atmospheric pollutants in passive sampling devices. Moreover, Ca-based materials are also used and tested as active support for palladium in the catalytic hydrogenation of aldehydes.

Passive samplers, initially developed and used for workplace air, have been found to be useful and cost-effective alternatives to conventional pumped samplers for monitoring ambient, indoor and personal exposures at low concentrations of analyte. In particular, passive samplers have been recognized as a valuable tool in environmental monitoring when the average, instead of the real time, pollutant concentration is the object of the monitoring. Respect to active samplers, passive ones can easily provide the measurement of time-weighted average (TWA) concentration which represents a fundamental part of the ecological risk assessment for chemical stressors. In contrast to active samplers where air is brought into contact with a detector or collector device by means of a pump, passive samplers depend on diffusion process which allows the interaction of the pollutant with the collector. Diffusion driving forces and separation mechanisms are based on the difference in the

chemical potentials of trapped and non-trapped analytes.

In particular, diffusive sampling relies on the principles of Fick's first law which can be expressed as $J= D/l(\rho_1 - \rho_2)$ where J = diffusive flux, D = diffusion coefficient of analyte, l = length of static air layer in the sampler, ρ_1 = concentration of the given analyte at the beginning of the diffusion layer (l=0) and ρ_2= concentration of the given analyte at the end of the diffusion layer.

The thesis is organized in the following sections.

Chapters 1 and 2 briefly describe applications of Ca-based materials in industrial processes and catalytic reactions.

In Chapter 3.1 is reported the synthesis and characterization of a new class of calcium based sorbent materials for the quantification and possibly the removal of NO_x from the atmosphere. Particularly, various CaO/Mayenite ($Ca_{12}Al_{14}O_{33}$) substrates having different weight ratio (w/w) composition, were synthesized and characterized. Their reactivity towards NO and NO_2 was evaluated by means of several experimental techniques: FT-IR and XRD were used to characterize the species formed during the sorption process, whereas IC and TGA analysis provided information about the dynamics of the sorption process itself. The hydration reaction occurring on the substrate before NO_x sorption has also been considered. Finally, the performance and the reliability of the

CaO/mayenite materials in field measurements by incorporating the substrate in a passive sampler device were tested. The simultaneous sorption of atmospheric NO_2 and NO has been investigated and the role of the carbon dioxide in the NO_x – CO_2 exchange reactions has been assessed.

In Chapter 3.2 is reported, the analysis of the carbon isotope composition ($\delta^{13}C$) which was performed for the first time in different urban and extra urban environments on atmospheric carbon dioxide collected by means of a new passive calcium–aluminium oxide-based sampler device.

$CaO/Ca_{12}Al_{14}O_{33}$ 75:25 w/w was used to determine stable carbon isotope ratios ($\delta^{13}C$) in the atmosphere, after atmospheric CO_2 sampling. Stable carbon isotopes ($\delta^{13}C$) have proven to be useful geochemical markers and were employed to study air pollution since the 1980s. The information on the isotopic composition of CO_2, together with standard analytical determination on its concentration, has been extensively used for characterizing the carbon dioxide atmospheric budgets and its biogeochemical origins. The isotopic composition of CO_2 also provides a powerful tool for assessing sources and sinks of carbon, at local, regional, and global scales. At the local scale, in particular, the isotopic composition of fossil fuel emissions has been used to trace back the fuel sources and distinguish them from the emissions

generated by the biological activity in the urban areas.
Field measurements were conducted in three environments characterized by different carbon dioxide sources. In particular, the environments under consideration were a rather heavily trafficked road, where the source of CO_2 is mostly vehicle exhaust, a rural unpolluted area, and a private kitchen where the major source of CO_2 was gas combustion.
In Chapter 3.3 it is described the incorporation of H^- anions into the mayenite framework under mild conditions compared to those reported in literature. Surprisingly mayenite hydrides without any metal loading was observed to be already active in the reduction of benzaldehyde to benzyl alcohol. Furthermore the loading of such active support with palladium resulted in an highly active and selective catalyst for the catalytic reduction of aldehydes. The evaluation of catalytic activity towards hydrogenation of benzaldehyde and cinnamaldehyde was explored giving intriguingly results in terms of activity and selectivity.

In conclusion, Appendix A is dedicated to the “Dottorati in azienda” project based on a brief research experience in Cleprin srl, a leader company in the production of detergents for professional use where an innovative chemical formulation was developed for household waste management.

CHAPTER I

1.1 Employment of Ca-based sorbent in industrial and environmental field

1.1 Carbon dioxide capture from anthropogenic sources

Carbon dioxide is the major contributor of greenhouse effect. To mitigate the greenhouse gas impact, it is important to sequester CO_2 from fossil-fuel plants, which account for about one-third of all anthropogenic CO_2 emissions[(1)]. Much of the work concerned the separation of CO_2 from methane for the purification of natural gas[(2)]. Several different approaches have been proposed to remove CO_2 from flue gases on a large scale[(3)], and selective adsorption or chemisorption on solids media are well known[(4)]. Different materials have been prepared and tested as carbon dioxide sorbent[(2)]. In Figure 1.1 a panoramic of some CO_2 sorbent materials is reported.

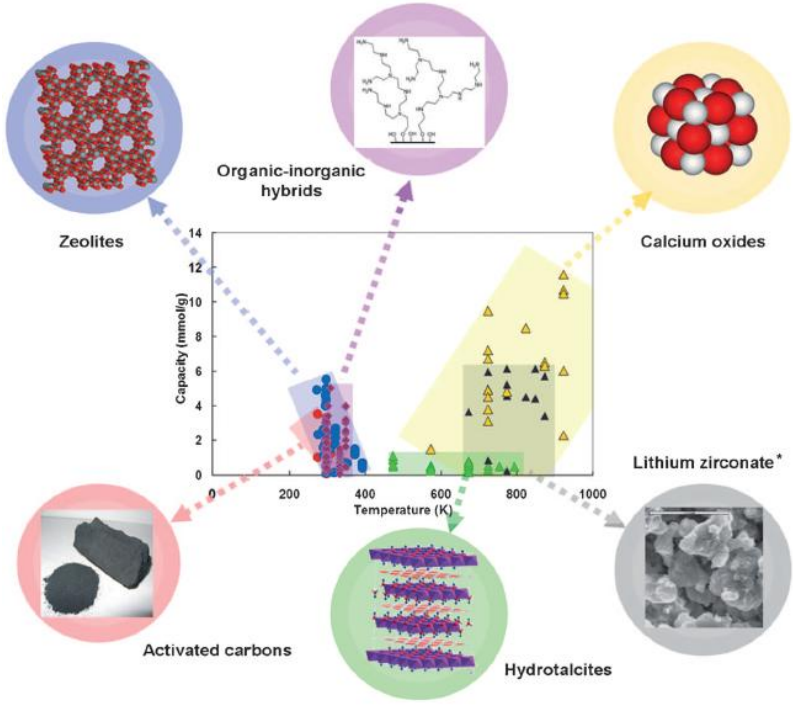

Figure 1.1 CO_2 sorbent materials.

The acidic nature of CO_2 facilitates adsorption on the basic sites of some metal oxides, especially those with a low charge/radius ratio. This group of materials includes alkaline metal oxides (Na_2O, K_2O) and alkaline earth metal oxides (CaO, MgO) on which CO_2 molecules can be adsorbed forming mono or multidentate species. Particularly, calcium oxide has been widely used as sorbent for CO_2 as reported in literature[5,6]. One mole of CaO reacts with a stoichiometric equivalent of CO_2 to form the correspondent carbonate through the following exothermic reaction:

$$CaO_{(s)} + CO_{2(g)} \longrightarrow CaCO_{3(s)}$$

In large scale CO_2 capture applications, these materials are thought to be advantageous compared to other adsorbents on account of the low cost and wide availability of precursor such as limestone and dolomite[7].

1.2 Carbon dioxide adsorption capacities of CaO

Based on the stoichiometric carbonation reaction of CaO, the maximum theoretical amount of adsorbed CO_2 is 17.8 mmol/g but typical capacities reported in literature are lower than this value and also they are still higher than those of other inorganic chemisorbents[8]. Barker demonstrated that CO_2 adsorption capacities of calcium oxide powder varied with changes in particle sizes and surface areas [9]. In addition, also the type and the composition of precursors influence the adsorption properties of calcium oxide-based adsorbents. Another important characteristic of CaO is its applicability in CO_2 adsorption-desorption cycles at high temperature in industrial processes. In fact, the reversible carbonation and decarbonation reactions of calcium oxide and CO_2 to produce $CaCO_3$ provide an interesting approach for CO_2 capture and separation from high-temperature gas streams, such as flue gas and gas streams encountered in coal gasification, fuel cell

applications, and chemical heat pumps[10]. Generally calcium oxide based adsorbents suffer from a rapid CO_2 capture capability during the repletion of carbonation/calcinations cycles due to pore blocking and adsorbent sintering. Experimental tests have demonstrated that the main factor for calcium oxide degradation was not adsorbent sintering but the blockage and collapse of the pore structure.

Extensive efforts have been made to enhance the stability of calcium oxide particulates by modifying their material properties, particularly, increasing surface area and preparing a more stable pore structure. The direction of this research can be categorized into four strategies: techniques using rigid supports, use of additives, preparation of nanoparticles and use of different synthetic precursors [5]. The first method is based on the concept of employing a rigid porous material as carrier for the calcium oxide species. Feng [11] prepared CaO particles in an inert alumina support. In the second method, additives were incorporated in the calcium oxide precursors to improve the adsorbent stability by preventing sintering of the particles during the regeneration stage[12]. The third technique is to reduce the particle size of the adsorbent down to the nanometer scale[13]. Finally, the fourth technique is based on the use of new synthetic precursors that can produce adsorbent materials with a rich micropore structure[14].

Li and its collaborators have prepared a new kind of Ca-based regenerable CO_2 absorbent, $CaO/Ca_{12}Al_{14}O_{33}$, on the basis of the integration of CaO, as solid reactant, with a composite metal oxide $Ca_{12}Al_{14}O_{33}$, as a binder, to applying it to repeated calcinations/carbonation cycles[15]. The use of the composite metal oxide has significantly improved CO_2 absorption capacity and cyclic reaction stability compared with other Ca-based absorbents. To prepare this new substrate authors propose a new interesting synthetic technique. High-reactivity absorbent is prepared mixing weighted amount of aluminium nitrate enneahydrate $[Al(NO_3)_3*9H_2O]$ and the powder calcium oxide into a mixture of 2-propanol and water in order to obtain a material with CaO and $Ca_{12}Al_{14}O_{33}$ weight ratio of 75/25%. The mixture is stirred at 75°C and dried at 120°C before being calcined at 500°C in air. By this method, 2-propanol, water and nitric acid in the solution can be evaporated off in different stages, thereby offering the production of a fine porous powder. These particles are dried at 120°C and calcined in air at 800°C. From a mechanistic point of view the hydration and calcinations of CaO and aluminium nitrate consists of many physical processes and chemical reactions. When CaO is added into water, the reaction of hydration changes CaO into $Ca(OH)_2$. The solution of aluminium nitrate and 2-propanol is mixed with

$Ca(OH)_2$ ultrafine particles with stirring at constant temperature. The addition of 2-propanol makes the particle size distribution of the hydration product $Ca(OH)_2$ more uniform. When the sample is calcined at 500°C, $Ca(OH)_2$ decompose to CaO. At the same time, aluminium nitrate begins to decomposes and generate Al_2O_3 according to the following reaction:

$$4Al(NO_3)_3 \longrightarrow 2Al_2O_3 + 12NO_2 + 3O_2$$

The penetration of aluminium nitrate into particles enables more porosity during the process of decomposition of aluminium nitrate. When the sample is calcined at higher temperature, CaO and Al_2O_3 inside the particle react to generate a new kind of material, $Ca_{12}Al_{14}O_{33}$:

$$12CaO + 7Al_2O_3 \longrightarrow Ca_{12}Al_{14}O_{33}$$

Schematic diagram of hydration preparation of absorbent is shown in figure 1.2.

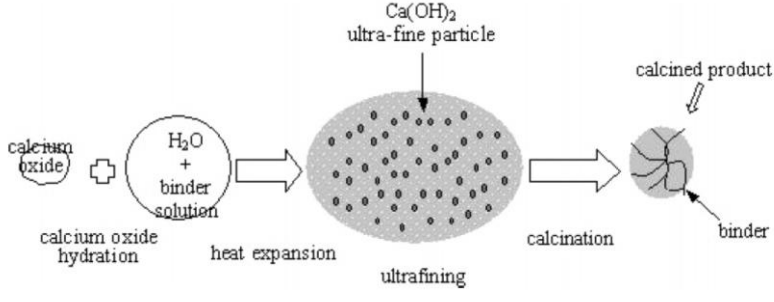

Figure 1.2 CO_2 absorbent preparation.

XRD analysis of the calcined samples confirms that only CaO

and $Ca_{12}Al_{14}O_{33}$ exist as shown in figure 1.3.

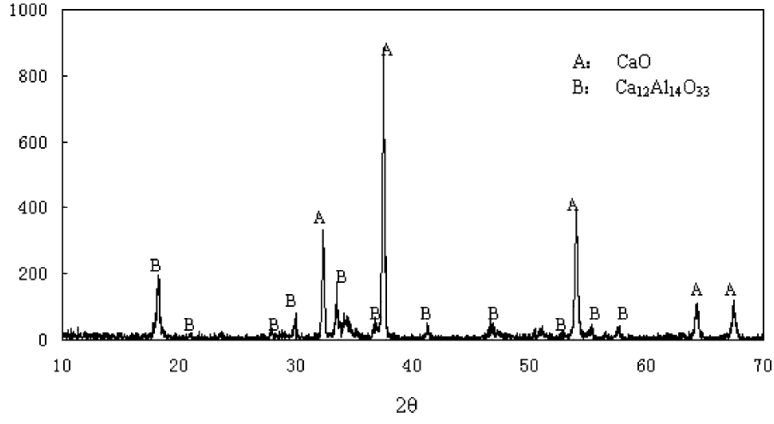

Figure 1.3 XRD image of the new absorbent $CaO/Ca_{12}Al_{14}O_{33}$(75/25%wt).

The new formed material during the cycles of carbonation/calcination acts as a binder and does not take part in the reaction and the absorbent shows a stable and high CO_2 absorption capacity as shown in figure 1.4.

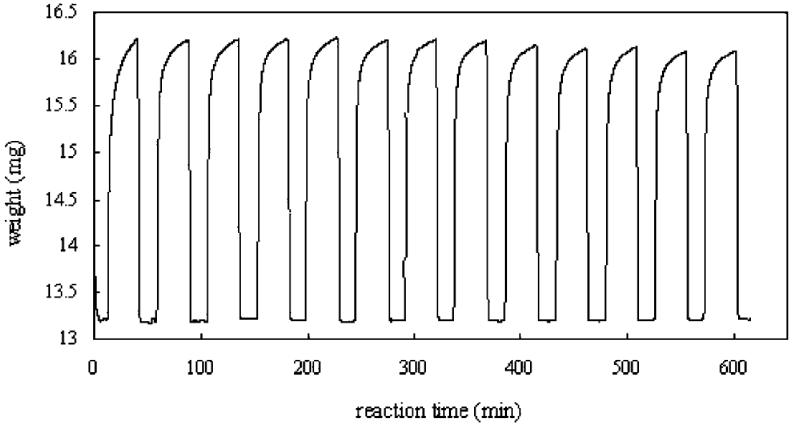

Figure 1.4 Carbonation/calcination cycles of $CaO/Ca_{12}Al_{14}O_{33}$.

1.3 NO_x uptake on alkaline earth oxides

The components of the polluting emission gases formed by the combustion of biomass and fossil fuels are mainly nitric oxide (NO) and nitrogen dioxide (NO_2) which are collectively named NO_x. NO is the primary form in combustion products (typically 95% of total NO_x). NO_x are the source of severe environmental problems such as acid rain, smog formation, global warming, and ozone layer weakening. For the past 30 years, great efforts have been made in research directed to find solutions for the NO_x problem. NO_x is produced not only by burning of fuels and biomass but also by lightening, oxidation of NH_3 (produced by microbial decomposition of proteins in the soil), and volcanic activity. Another nitrogen oxide that is relevant due to its important role in atmospheric pollution is N_2O. It is produced mainly in the nature by microbial activity. However, its level in the atmosphere continues to increase mainly due to anthropogenic activities. N_2O is converted into N_2 and NO in the stratosphere and it contributes to the destruction of the earth's protective ozone layer and to the green house effect.

Generally, two different approaches are considered to reduce NO_x concentrations in atmosphere and its related environmental problems such as acid rain, photochemistry smog, ecc. A first approach consists in modifying the

operational conditions to decrease the NO_x formation. Among new developed technologies, the furnaces with low production of NO_x represent an important contribution. A second approach consists in destroying or allowing NO_x to react with other reagents, making it possible to eliminate them or to modify them. Different material types are reported for the sorption of nitrogen oxides: some can adsorb NO or NO_2 separately, but others can adsorb both of them. For reviewing, they were classified as follow: metal oxides, spinels, perovskites, zeolites, carbonaceous materials, and heteropolyacids. During the last forty years, several technologies were developed to control and diminish the NO_x emissions in the environment[16]. Many alkaline earth metal oxides were synthesized and tested as NO_x sorbents (BaO, MgO, CaO, $BaAl_2O_4$, $BaAl_{12}O_{19}$). As an example, BaO was tested to selectively react with NO_2 through an intermediate oxidation of NO catalyzed by noble metals (Pd and Pt), to yield nitrates as the final product[17]. This system has been regarded as one of the most promising solution for the control of exhaust emissions in diesel engine devices. In order to evaluate possible interfering reactions with the sorption process, further experiments were performed to check the formation of parasite species like carbonates and sulphates, on the metal oxides surface[18]. By following this approach,

nitrate species (bulk and surface nitrates) were characterized after the exposure of different metal oxides to NO_2 and the behavior of several alkaline earth oxides (SrO/γ-Al_2O_3, CaO/γ-Al_2O_3 and MgO/γ-Al_2O_3) was investigated[19,20]. The amount of the sorbed NO_x strongly depends on the sorption mechanism as well as on the physical properties of the sorbents and the sorbates.

In 2005, Li [15] developed a new Ca-based material for the sorption of CO_2 in industrial processes: CaO/$Ca_{12}Al_{14}O_{33}$ was obtained by integrating solid CaO with a composite metal oxide, $Ca_{12}Al_{14}O_{33}$ (Mayenite), acting as the binder. Mayenite is a nanoporous calcium aluminate prepared by calcination at about 1300°C of stoichiometric amount of calcium carbonate and alumina. Mayenite has an antizeolite-type structure with interconnected positively charged cages, which can host a variety of anionic species[21,22].

Recently, we succeeded in using CaO/$Ca_{12}Al_{14}O_{33}$ as a solid sorbent material in passive sampling devices for the determination of the atmospheric CO_2[23]. In this thesis I present the synthesis of different substrates with variable weight ratio CaO/$Ca_{12}Al_{14}O_{33}$, namely 75:25 w/w (CM75), 35:65 w/w (CM35) and pure mayenite (PM), capable to react simultaneously with NO and NO_2. A simple and economic sol-gel synthesis of mayenite is also described. We further

characterized the reactivity of mayenite by investigating the influence of water surface sorption. Hydration phenomena were found to play an important role in the process of NO_x sorption and their subsequent conversion to nitrite and nitrate species. IR and TGA techniques were used to characterize the reaction products. A simple method to quantify the uptake of NO_x is also devised, also taking into account the interference of CO_2 in environmental conditions. Finally I present a possible application of the calcium oxide based sorbents for the simultaneous determination of atmospheric NO and NO_2 with passive sampling devices [24].

1.4 Desulfurization processes using Ca-based sorbent

Coal-fired power generation will continue to play a key role in power supply because the estimated coal reserves are very large and the cost of coal is lower than that of other energy sources. In such scenario, SO_2 emission from coal combustion causes many serious problems. Wet, semi-dry and dry desulfurization processes have been found to be very effective for SO_2 removal. Particularly, dry processes using Ca-based adsorbents[25] have low costs, needs no water, and produces the valuable byproduct $CaSO_4$. At the typical combustion temperature, 800-900°C, CaO produced by $CaCO_3$ decomposition reacts with SO_2 and or with SO_3 to form $CaSO_4$. One of the most economical desulfurization processes is the direct limestone injection method but the efficiency of this method is very poor because of the low calcium utilization rate and the short-time residence time of lime. Li et al.[26] have developed a new method for preparing low cost, highly active sorbent by mixing CaO and fly ash in water. The mixed slurry was dried at 85°C and the dried cake obtained was crushed to regain the original fine powder. Sorbent shows high activity in the dry-desulfurization process achieved an 83% SO_2 removal rate without any humidification as shown in figure 1.5 . They also consider NO and NO_2 effects on SO_2 removal rate.

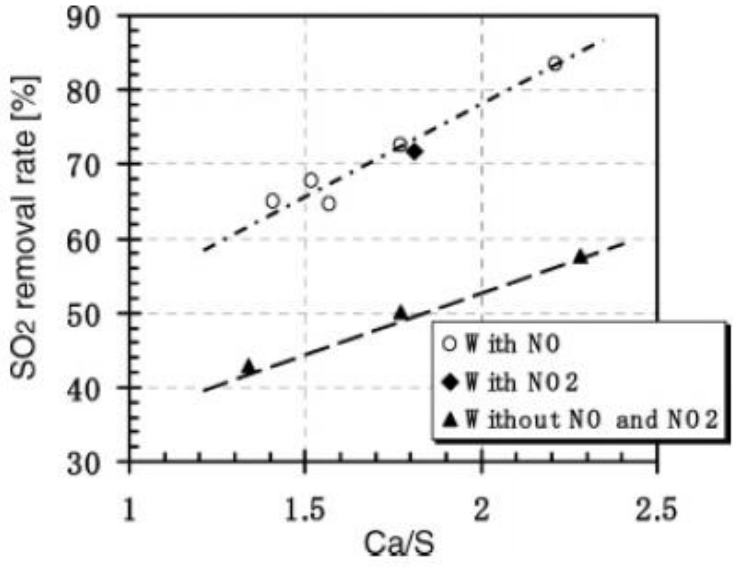

Figure 1.5 SO_2 removal using Ca-based sorbent.

Chen et al.[27] synthesized a new sorbent consisting of only mayenite ($Ca_{12}Al_{14}O_{33}$) and found that this material reacts with SO_2 but the conversion achieved was much lower than that for limestone. Relying on these results, Pacciani[28] synthesized a composite material, CaO/ $Ca_{12}Al_{14}O_{33}$ 85:15% wt, into ways of enhancing the capture of SO_2 in a fluized bed coal-combustor. This sorbent revealed the presence of pores with diameters up to 10 μm and reacted uniformly, owing to these large pores, not susceptible to premature blocking.

Not only SO_2 was produced in coal-fired power plants but, it must be taken into account that the sulfur contained in coal reacts in the reducing atmosphere of a gasifier generating

H_2S. Desulfurization at higher temperatures (up to 1200 °C) would make a substantial contribution in improving the thermal efficiency of electric power generation which can be as much as 2-3%. Among the possible sorbents for H_2S removal at such high temperatures, calcium-based materials have the advantage of being cheap, abundantly available, and commonly used as bulk chemical. J. Adanez et al.[29] used five calcium-based sorbents of different nature: three limestones characterized by different porous structures, a dolomite, and a calcium hydroxide. Authors did not found a direct relation between chemical composition and sorbent reactivity and sulphur retention up to 70% was achieved only using calcium hydroxide, the dolomite and one of the three limestones. Figure 1.6 shows sulfur removal, obtained in the reactor as a function of Ca/S molar ratio for the five sorbents studied.

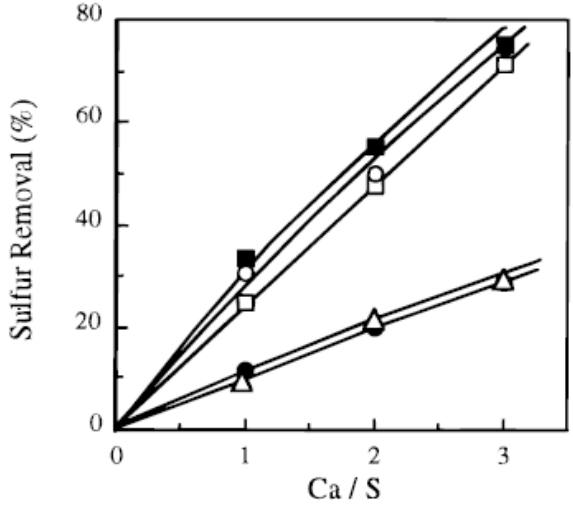

Figure 1.6 Effect of Ca/S molar ratio on sulfur removal.

As expected, an increase in the Ca/S molar ratio produced an increase in the sulfur removal, which was different for each sorbent used. These sorbents showed the highest porosities and the highest average pore diameter in their calcines. A direct relation between porous structure and H_2S removal can be inferred from these results.

References

(1) H. Lu et al., Ind. *Eng. Chem. Res.* **2006**,45,3944-3949
(2) S. Choi et al., *ChemSusChem* **2009**,2,796-854
(3) B. Balasubramanian et al., *Chem. Eng. Sci.* **1999**,54,3543-3552
(4) Yang R.T. et al., *Gas separation by adsorption processes*, Imperial college press, London, **1997**.
(5) G. Grasa et al., *Energy Fuels.* **2007**,21,3560-3562
(6) G. Grasa et al., *Ind. Eng. Chem. Res.* **2006**,45,8846-8851
(7) E. Oliveira et al., *Sep. Purif. Technol.* **2008**,62,137-147
(8) A. Ortiz et al., *Ind. Eng. Chem. Res.* **2001**,40,5102-5109
(9) R. Barker, *J. Appl. Chem. Biotechnol*. **1974**,24,221-227
(10) E. Reddy et al., *J. Phys. Chem. B* **2004**,108,7794-7800
(11) B. Feng et al., *Energy Fuels* **2006**,20,2417-2420
(12) J. Ida et al., *Environ. Sci. Tech.* **2003**,37,1999-2004
(13) S. Wu et al., *Ind. Eng. Res. Chem.* **2008**,47,180-184
(14) H. Gupta et al., *Ind. Eng. Res. Chem.* **2002**,41,4035-4042
(15) Z. Li et al., *Energy Fuels* **2005**,19,1447-1452
(16) M. Gomez-Garcia et al., *Environ. Int.* **2005**,31,445-467
(17) E. Fridell et al., *Catal. Lett.* **2000**,66,71-76
(18) S. Hodjati et al., *App. Catal. B Environ.* **1998**,19,221-232
(19) J. Szanyi et al.,*J. Phys. Chem. B* **2005**,109,27-29
(20) C. Verrier et al., *Catal. Today* **2008**, 136,121-127
(21) L. Palacios et al., *Inorg. Chem.* **2007**,46,4167-4176
(22) M. Ruszak et al., *Catal. Lett.* **2008**,126,72-77
(23) R. Cucciniello et al., *Atmos. Environ.* **2012**,60,82-87
(24) A. Proto et al. Campionatori di inquinanti in aria **2008**, Italian Patent MI2008A001318
(25) N. Matstushima et al., *Environ. Sci. Technol.* **2004**,38,6867-6874
(26) Y. Li et al., *Energy Fuels* **1999**,13,1015-
(27) G. Chen et al., *Ind. Eng. Chem. Res.* **2010**,49,1450-1456
(28) R. Pacciani et al., *Ind. Eng. Che. Res.* **2009**,48,7016-7024
(29) J. Adanez et al., *Energy Fuels* **1998**,12,726-733

CHAPTER II

2.1 Catalytic applications of alkaline oxides: The history of Mayenite ($Ca_{12}Al_{14}O_{33}$)

2.1.1 Mayenite ($Ca_{12}Al_{14}O_{33}$): structure and properties

The mineral mayenite, known for a long time as a major constituent of calcium aluminate cements was originally reported from the Eifel volcanic complex in Germany. Mayenite is an attractive material because it is thermodynamically stable with a relatively low melting point, 1390-1400°C.

Mayenite, labeled as C12A7, is a mesoporous calcium aluminate ($12CaO*7Al_2O_3$) which has a positively charged lattice framework $[Ca_{24}Al_{28}O_{64}]^{4+}$ per unit cell that includes two molecules and twelve cages with a free space of 0.4 nm in diameter. The chemical formula for the unit cell may be represented as $[Ca_{24}Al_{28}O_{64}]^{4+}$ $*2O^{2-}$ and it has a body centered cubic crystal structure belonging to the *I*-43*d* space group with a = 11.989 Å and Z =2.

The remaining two oxide ions O^{2-}, namely “free oxygen”, are trapped in the cages defined by the framework satisfying the overall electroneutrality condition. More in detail, the framework of mayenite is composed by interconnected cages similar to those found in zeolites and the cage shows

entrances of 0.1 nm in diameter that control mass transport between the inner cages and the outside[1]. A fundamental difference between mayenite and conventional zeolites is the charge polarity of the lattice framework; cationic species are introduced to compensate for the negative charge caused by the substitution of Al^{3+} ion for Si^{4+} ion in the zeolites. On average each cage has a mean effective charge of +1/3, so the free oxygen anions compensate this positive charge of the framework and are coordinated to the six Ca^{2+} cations forming the cage walls along with the Al^{3+} cations. The oxygen ions are loosely bound to the framework because the spacing between them and the closest Ca^{2+} is about 1.5 times bigger than the sum of their effective radii.

Due to the space confinement, the guest species are limited to mono or diatomics such as O^{2-}, O^{-}, O_2^{-}, O_2^{2-}, OH^{-}. Mayenite derivates were obtained exchanging the O^{2-} anions for other different ions, such as OH^{-} [2], $F^{-}$and Cl^{-} [3], O_2^{-} [4] and H^{-} [5].

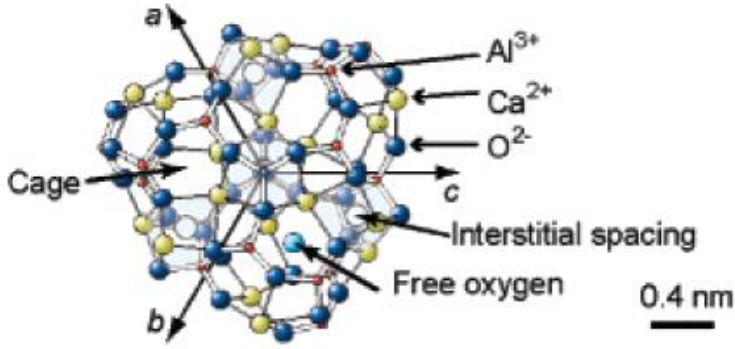

Figure 2.1 Part of the crystal structure of mayenite viewed from the <111> direction.

Generally, low surface area mayenite (S_{BET}<10m^2/g) was prepared by calcination of stechiometric amount of $CaCO_3$ and Al_2O_3 at temperatures around 1300°C[6]. Indeed, this material shows high thermal stability and was employed by Li[7] as binder in a new CO_2 sorbent material increasing the cyclic reaction stability over multiple carbonation-calcination cycles.

Matshiushi et al. reported the conversion of mayenite (C12A7) , an insulating oxide crystal, into a persistent electrical conductor (C12A7:H) after heated at 1300°C in hydrogen atmosphere upon UV illumination[8]. Authors show that although the UV-illuminated C12A7:H shows optical absorption in the visible region due to two absorption bands centered at 0.4 and 2.8 eV, transmission loss in the visible

range remains at only a few % for the 200 nm thick films. Furthermore, the conductivity is eliminated by annealing at 330°C , and this cycle of emergence of UV-induced conductivity and thermal restoring is reversible unless the sample is heated to 500°C. Therefore, C12A7:H thin film may be used for the direct optical writing of rewritable conducting patterns in this insulating transparent media. On the basis of the anion encaging nature of C12A7, it was suggested that the conductivity arising in C12A7:H is due to carrier electron generation by photoexcitation of H^- captured in the subnanometer-sized cage of C12A7[9]. This new material has not been previously used in catalytic reactions involving hydrides.

2.2 Mayenite as active catalyst support: an overview

As a matter of fact, ionically conducting ceramics have received increasing interest as active catalyst supports[10]. Furthermore, the ability of storing oxygen ions in the nanocages is a unique properties of mayenite and several works show its application in catalytic process as oxidant species[10]. The most promising for catalysis is the fact that the encaged oxygen species can migrate between the surface and the bulk. They can be gradually released at elevated temperatures or stored. Therefore, the reported catalytic

activity properties of mayenite have often been associated with its strong oxidation ability.

Indeed, the use of mayenite as substrate for Ni catalyst was reported for biomass tar steam reforming in a fixed bad reactor using toluene as tar destruction model compound. 1% Ni on mayenite shows excellent performances either in absence and presence of H_2S.

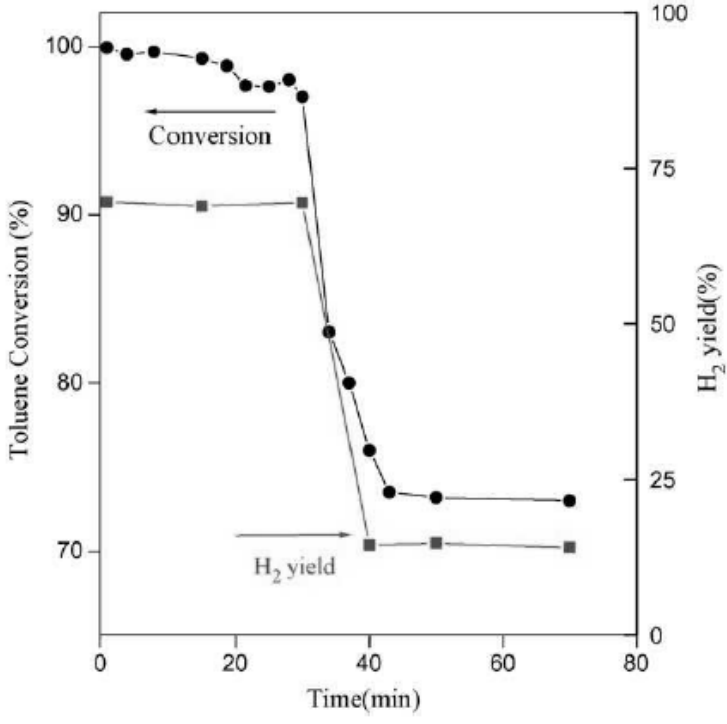

Figure 2.2 Toluene conversion and H_2 yield vs time on Ni/Mayenite 5% wt at 800°C.

Moreover, $Ni/Ca_{12}Al_{14}O_{33}$ showed excellent sustainability

against coke formation due to the "free oxygen" in the catalyst. O_2^{2-} and O_2^- inhibit Ni poisoning by sulphur incorporation in the cages[11].

Hosono et al. have investigated the partial oxidation of methane to CO and H_2 over mayenite promoted metals such as Ni, Co, Pt, Rh and Ru[12]. On Ni, Pt and Pd/C12A7, this reaction readily happened at temperatures as low as 500°C and attained thermodynamic equilibrium. Mayenite without any metal catalyst shows at the same time good performance in the partial oxidation of methane as shown in figure 2.3. Furthermore, ethane and ethene were also formed at temperatures higher than 650°C (10% selectivity at 800°C) due to the existence of active oxygen (O^-, O^{2-}, O_2^{2-}) in C12A7 which readily activated methane into radicals and caused their coupling.

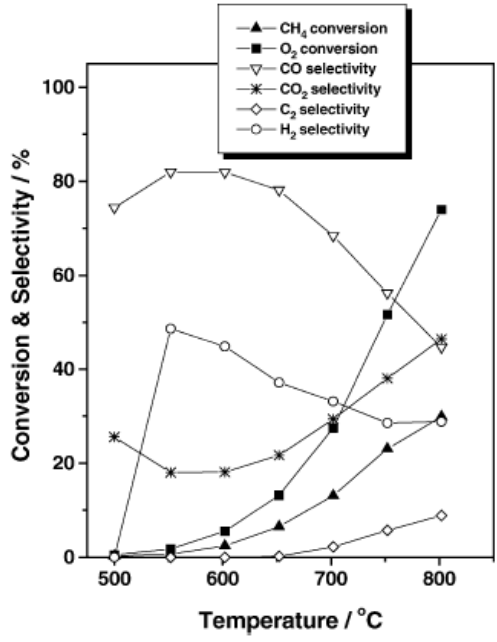

Figure 2.3 Conversion and selectivity of methane partial oxidation to syngas over mayenite.

When mayenite was promoted by Ni, Pt and Pd, partial oxidation of methane into CO and H_2 readily proceeded even at 500°C.

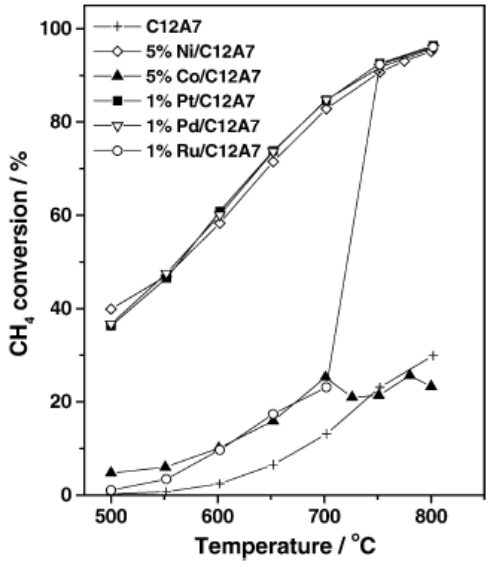

Figure 2.4 CH_4 partial oxidation to syngas over unpromoted and promoted mayenite as a function of temperature.

In 2007, Ruszak et al.[13] studied the high temperature decomposition of nitrous oxide, N_2O, over mayenite. This application is very interesting because in the nitric acid plants, N_2O is an indesiderable by-product and two types of deN_2O technologies are available on market: a non catalytic and a catalytic one. The non catalytic technique involves the thermal destruction of N_2O and mayenite support can be used in this context. Authors show an appreciable conversion of N_2O above 600°C and upon reaching the process temperature of 900°C the decomposition of nitrous oxide achieved ca. 90%. From a mechanicistic point of view, for the N_2O

decomposition over oxide catalysts not containing transition metal ions the anionic redox mechanism initiated by the oxygen atom transfer was proposed. In this context the peculiar feature of mayenite, with its large capacity for storage of the subsurface oxygen species, opens two interesting mechanistic pathways. They consist in suprafacial recombination of surface peroxy ions and intrafacial recombination of surface peroxy with cage and surface oxygen species as also shown in figure 2.5:

$$O_2^{2-}{}_{(surf)} + O_2{}^{x-}{}_{(cage)} \longrightarrow O_2 + O^{2-}{}_{(surf)} + O^{x-}{}_{(cage)}$$

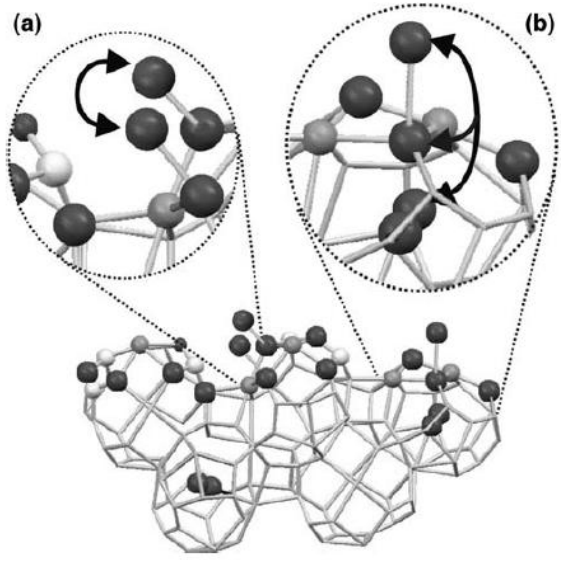

Figure 2.5 Suprafacial (a) and intrafacial (b) recombination of oxygen atoms produced upon dissociation of N_2O.

2.3 Ammonia synthesis using a stable mayenite electride as support for ruthenium

In 2003, the first inorganic electride, C12A7:e^- was synthesized utilizing mayenite. Electrides are materials that trap electrons at a stoichiometric concentration in the solid state. Notably, this material became the first stable electride in air at room temperature[(14)]. Mayenite electrides were prepared starting from the C12A7 crystals that were sealed in silica glass tubes under vacuum together with metal calcium shots, and heated at 700°C for several hours. The Ca treatment did not change the basic structure of the lattice framework of C12A7. The sample color changed from colorless to green, and finally to black, with increasing duration of Ca treatment. Authors demonstrate that electrons are injected in the C12A7 lattice by the Ca treatment in place of the free O^{2-} ions.

$$[Ca_{24}Al_{28}O_{64}]^{4+}*(O^{2-})_2 + 2Ca \rightarrow [Ca_{24}Al_{28}O_{64}]^{4+}*(4e^-) + 2CaO$$

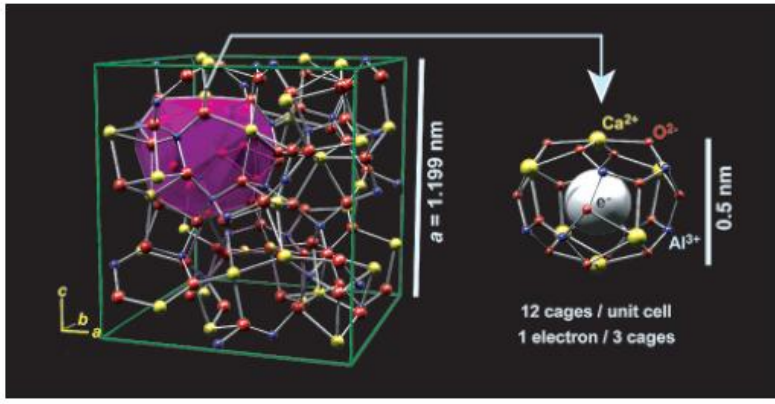

Figure 2.6 Crystal structure of the C12A7 electride.

Successively, in 2012, Hosono's research group used mayenite electrides in the ammonia synthesis as an electron donor and reversible hydrogen store[15] and in the pinacol coupling reaction in aqueous media[16].

More in detail, in the NH_3 synthesis mayenite electride acts as an efficient electron donor for a Ru catalyst. The electride has a high electron-donating efficiency and chemical stability, and does not exhibit H_2-poisoning because of its reversible hydrogen absorption/desorption capability, which results from its crystal structure.

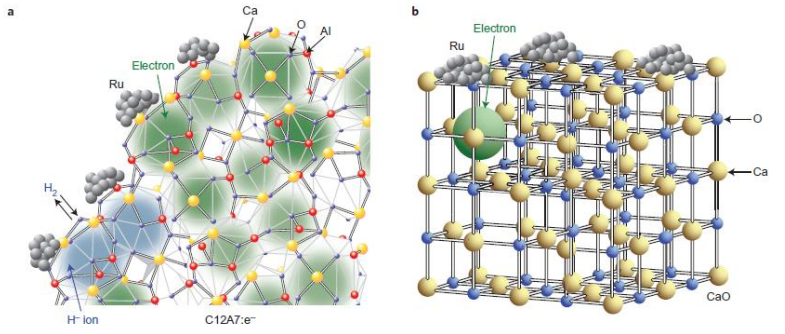

Figure 2.7 Ru/Mayenite electride catalyst.

Electrons encaged in C12A7:e^- are transferred to the Ru metal, and as a consequence, back donation from Ru with an excess electron density to the N_2 π^*-antibonding orbital is enhanced, which leads to a weakening of the N-N bond of adsorbed N_2. Although H_2 molecules are also adsorbed dissociatively on Ru surfaces, hydrogen adatoms readily spill over onto electride and are incorporated into the nanocages as H^- ions. This incorporation prevents hydrogen adatoms from poisoning the Ru surface. The activated nitrogen species react with H^- ions entrapped by C12A7 nanocages or with hydrogen adatoms on Ru to form ammonia. In the case of the former, H^- ions leave electrons in the cages and the resulting hydrogen species react with the activated nitrogen near the Ru-electride interface. The electrons encaged in the mayenite electride are used repeatedly during the reaction. Highly efficient ammonia synthesis is achieved with a catalytic activity that is an order

of magnitude greater than those of other previously reported Ru-loaded catalysts and with almost half the reaction activation energy.

Pinacol coupling reaction was conducted in aqueous media using mayenite electride. This reaction between two aldehyde molecules was investigated because the reaction is induced by the transfer of electrons from the chemical reagent to the aldehyde.

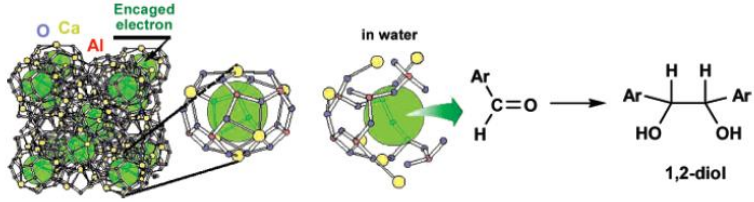

Figure 2.8 Pinacol coupling reaction promoted by mayenite electride.

When benzaldehyde and C12A7:e^- (mayenite electride) are mixed in water, the dark brown electride gradually dissolves and the mixture slowly becomes a white suspension. Hydrolysis of the white gel by aqueous HCl, followed by diethyl ether extraction produces 1,2 diphenylethyleneglycol, indicating that the pinacol coupling reaction took place as shown in figure 2.9.

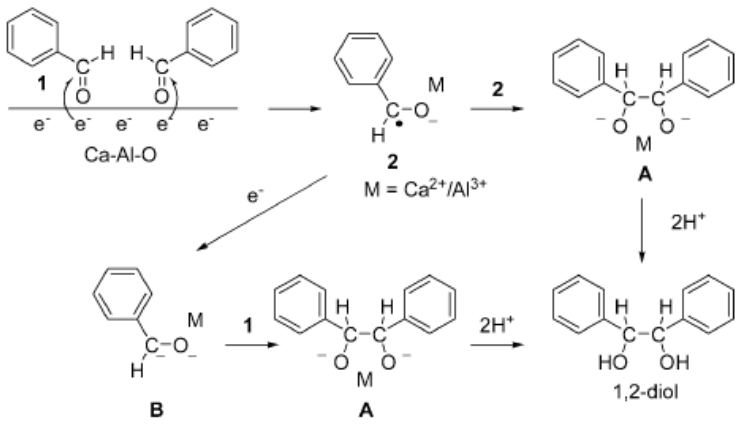

Figure 2.9 Mechanism of pinacol coupling promoted by C12A7:e^-.

The pinacol coupling is presumed to take place within the gel. The transfer of electrons to carbonyl carbon atoms of the aldehyde occurs on the surface of the C12A7:e^-. The formed anion radicals are concentrated within the gel layer and may be stabilized by coordination to metal cations (Ca^{2+} or Al^{3+}) in the gel or on the surface of the solid electride (**2**). Dimerization of the anion radical coordinated to the metal would form the pinacolate dianion (**A**), while one electron reduction of **2** and subsequent nucleophilic addition of the resulting dianion (**B**) to the carbonyl group of aldehyde would also yield **A**. Both of the C-C bond-forming reactions are possible in the pinacol coupling. The coordination of the intermediate to calcium and/or aluminum cations in the gel or on the surface serves to stabilize and concentrate them and to enhance the coupling in the presence of a large amount of

water.

References

(1) F. Huang et al. *Appl. Phys. Lett.* **2005**, 86, 114101
(2) K. Hayashi et al. *J. Phys. Chem. B* **2005**, 109, 11900-11906
(3) K. Hayashi et al. *J. Phys. Chem. B* **2007**, 111, 1946-1956
(4) K. Hayashi et al. *J. Am. Chem.Soc.* **2002**, 124, 738-739
(5) K. Hayashi et al. *Nature* **2002**, 419, 462-465
(6) S. Yang et al. *Chem. Mat.* **2004**, 16, 104-110
(7) Z. Li et al., *Energy Fuels* **2005**,19,1447-1452
(8) H. Kamioka et al. *J. Photochem.Photobiol. A: Chem.***2004**,166,141-147
(9) S. Matsuishi et al. *J.Am.Chem.Soc.* **2005**, 127, 12454-12455
(10) P. Vernoux et al. *Chem. Rev.* **2013**, 113, 8192-8260
(11) C. Li et al. *App. Cat. B: Environ*. **2009**, 88, 351-360
(12) S. Yang et al. *Appl. Cat. A: Gen*. **2004**, 277, 239-246
(13) M. Ruszak et al. *Cat. Lett.* **2008,** 126, 72-77
(14) S. Matsuishi et al. *Science* **2003**, 301, 626-629
(15) M. Kitano et al. *Nature Chem.* **2012**, 4, 934-940
(16) H. Buchammagari et al. *Org. Lett.* **2007**, 9, 4287-4289

CHAPTER III
Experimental part

3.1 Development of Ca-based sorbent for atmospheric NO_x sampling

3.1.1 Preparation of $CaO/Ca_{12}Al_{14}O_{33}$ substrates

$CaO/Ca_{12}Al_{14}O_{33}$ sorbent substrates with two different w/w ratio, namely 75:25 (CM75) and 35:65 (CM35) and pure Mayenite (PM) were synthesized. $CaO/Ca_{12}Al_{14}O_{33}$ was prepared following the procedure proposed by Li et al.[1] , as follows: 56.8 g of aluminium nitrate nonahydrate, $Al(NO_3)_3 \cdot 9H_2O$, and 26.2 or 52.4 g, depending on the chosen w/w ratio, of calcium oxide were added into a mixture of distilled water (1.5 L) and 2-propanol (260 mL). This solution was stirred for 1 hour at 75°C and successively dried at 120°C for 18 hours, the solid was then calcined at 500°C for 3 hours in the air to obtain a fine and porous powder. Distilled water was added to the powder and the obtained paste was dried at 120°C for 2 h and finally recalcined in air at 800°C for 1.5 h.
PM was prepared by sol-gel synthesis: 69.6 g of calcium nitrate tetrahydrate, $Ca(NO_3)_2 \cdot 4H_2O$, and 111.6 g of $Al(NO_3)_3 \cdot 9H_2O$ were dissolved in 1.5 L of distilled water. The mixture was heated on a hot plate at 60 °C, then 5 g of citric acid, $C_6H_8O_7$, were added. The citrate-nitrate mixture

was heated and vigorously stirred at 90 °C until a gel was formed (about 12 hours). The resulting gel was placed in a drying oven at 130 °C until a cake-like structure was obtained. The solid was then crushed into fine powder by using the agate mortar and pestle and finally placed into a furnace at 1000 °C in air for 4 hours.

In order to evaluate the influence of the hydration process on NO_x sorption, an aliquot of all the synthetized materials was hydrated through exposure to water vapour in a closed system for 7 days.

All reagents were purchased from Sigma Aldrich (reagent grade) and used without further purification.

3.1.2 Substrates characterization

All the crystalline structures of the dry and hydrated materials were characterized before exposure to NO_x by means of the X-ray diffraction (XRD) technique. XRD patterns were obtained on a Bruker D8 Advance automatic diffractometer operating with a nickel-filtered CuKα radiation. Data were recorded in the 2θ range of 4-80° with the resolution of 0.02°. Figure 4.1 shows the typical X-ray diffraction patterns of the synthesized PM, panel (A), CM75, panel (B), and CM35, panel (C).

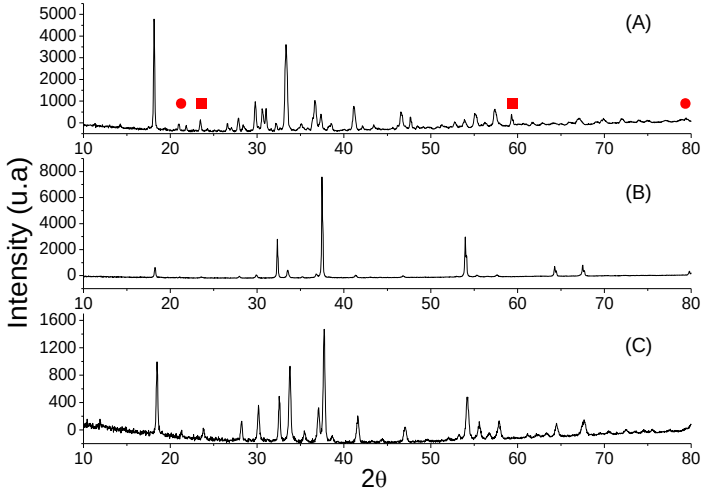

Figure 3.1 X-Ray diffraction patterns of (A) mayenite; (B) CaO/Mayenite 75:25 w/w and (C) CaO/Mayenite 35:65 w/w. Symbols in panel (A) reveal the presence of two spurious phases in the structure of mayenite, namely ● $Ca_3Al_2O_6$ and ■ $CaAl_2O_4$.

PM was indexed within I-43d space group. Together with the major mayenite phase, two typical spurious minor phases, namely $Ca_3Al_2O_6$ and $CaAl_2O_4$[(2)] were detected in the XRD pattern as indicated by circles and a squares, respectively, in the panel (A) of Figure 3.1. Panels (B) and (C) show the typical spectra of dehydrated substrates CM75 and CM35 with the characteristic peaks of CaO and $Ca_{12}Al_{14}O_{33}$. In hydrated samples, characteristic signals of calcium hydroxide could also be detected. $Ca(OH)_2$ is formed through the reaction of CaO with water vapor.

3.1.3 NO_x sorption experiments

NO_2 was produced from the lead nitrate, $Pb(NO_3)_2$, thermal decomposition at 500 °C while 60 mg of NO were obtained from the reaction of 250 mg of sodium nitrite with 3 mL of a solution of iron sulphate (1.2 M) and sulphuric acid (1.8 M), according to the following reaction[4]:

$$2NaNO_2 + 2FeSO_4 + 3H_2SO_4 \longrightarrow 2NO + Fe_2(SO_4)_3 + 2NaHSO_4 + 2H_2O \quad (1)$$

The sorption tests were carried out in a closed system composed by two glass flasks connected through a tube. In one of the two flasks the NO_x formation reaction took place, while in the other was poured the sorbent material. In each experimental run 1.0 g of sorbent material was saturated with NO_2 (3.3 mM) or NO (0.8 M) at 25 °C for 48 h. NO sorption experiments were conducted in a N_2 inert atmosphere in order to inhibit the NO oxidation to NO_2. At the end of each experiment, samples were preserved in N_2 atmosphere before analysis.

3.1.4 Thermal analysis

Thermal analyses were conducted in order to check the hydration and carbonation degree of the various samples. The mass sample evolution was recorded, as a function of temperature, by using a Netzsch TG 209 apparatus. The analyses were carried out on samples with a mass of about 20 mg placed inside an alumina crucible. The sample temperature was then increased with heating rate of 10°C/min from room temperature up to 900°C under an inert atmosphere of nitrogen. The temperature of the sample and the reference were recorded by a platinum/rhodium thermocouple while a high-precision balance registered the weight loss due to the decomposition of the sample.

Thermal analyses were repeated three times in order to test samples homogeneity and also the reproducibility of the instrument.

The hydration reaction of mayenite forms different species, depending on the environmental temperature. The most common are calcium aluminate minerals such as monocalcium aluminate ($CaO{\cdot}Al_2O_3$) and monocalcium dialuminate ($CaO{\cdot}2Al_2O_3$). Mayenite also forms stable hydrates such as, tricalcium aluminate hexahydrate ($3CaO{\cdot}Al_2O_3{\cdot}6H_2O$) and aluminum hydroxide trihydrate

$(Al_2O_3 \cdot 3H_2O)$[5].

Figure 3.2 shows the thermograms for the three different hydrated sorbents. Several inflection points can be observed in the range 20 – 400 °C, most probably due to the loss of physically adsorbed water and to the partial dehydration of $Al(OH)_3$ to Al_2O_3[6]. However, the three curves indicate that the quantity of sorbed water depends on the CaO/Mayenite ratio and it is proportional to the CaO content. This phenomenon is due to the formation of $Ca(OH)_2$ from CaO, as also confirmed by the XRD analysis. As shown in the thermograms reported in Figure 2, the maximum level of sorbed water is 30% for all the sorbent materials, hydrated in the closed system. However, in open atmospheric conditions (humidity 70% average), while CaO/mayenite compounds can be easily hydrated, pure mayenite does not adsorb water even after ten days of exposure.

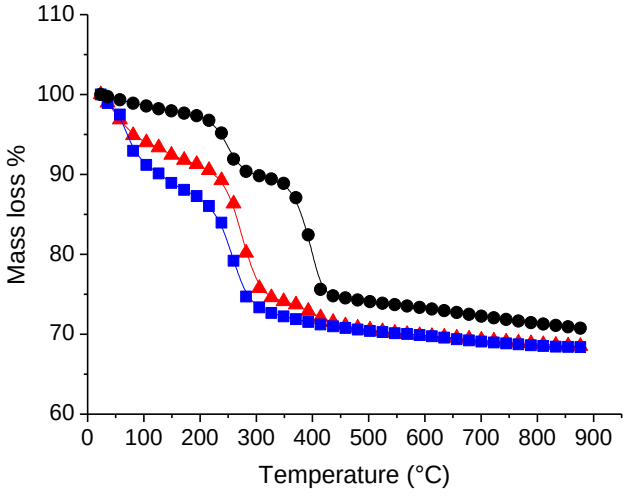

Figure 3.2 Thermograms of three different samples of sorbent materials after the hydration process in a closed system. ■ Mayenite; ▲ CaO/Mayenite 35:65 w/w; ● CaO/Mayenite 75:25 w/w.

3.1.5 Infrared characterizazion of the material after the exposure to NO_x

In order to characterize the NO_x species sorbed on CM75, CM35 and PM, FTIR spectroscopic measurements were carried out using a Vertex 70 FTIR spectrometer from Bruker equipped with deuterated triglycine sulfate (DTGS) detector and a Ge/KBr beam splitter. The frequency scale was internally calibrated to 0.01 cm^{-1} using a He-Ne laser. Infrared spectra in the middle range (4000–400 cm^{-1}) were acquired at a resolution of 2.0 cm^{-1} and at a scanning number of 32. The analyses were carried out on a pressed mixture prepared by using about 3 mg of sample in 100 mg of dried KBr. A sample of freshly prepared sorbent material was used as blank for the background correction.

Figure 3.3 and Figure 3.4 report the FTIR spectra for the dehydrated and hydrated CaO/Mayenite substrates, respectively, after the exposure to NO_2 (3.3 mM) or NO (0.8 M) at 25 °C for 48 h. In Figure 3.3 two typical sorption bands of nitrates (1385 and 1430 cm^{-1}) can be detected after the exposure of the dehydrated materials to NO_2 or to NO, while a band indicating the presence of nitrite ions (1271 cm^{-1}) can be detected only after the exposure to NO. However, the intensity of the signals is quite low for all the reported

scenarios, meaning that the reaction between substrates and NO_x is not very effective for the dry materials.

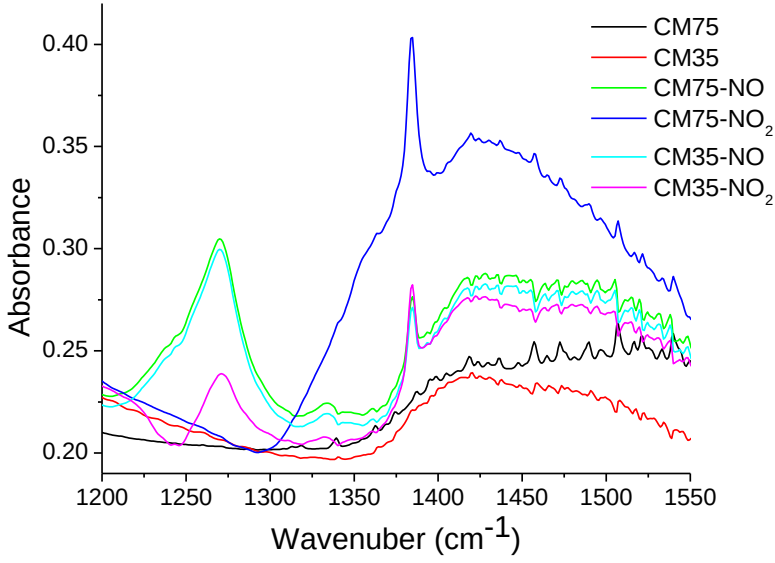

Figure 3.3 FTIR spectra of unhydrated CaO/Mayenite substrates after NO and NO_2 adsorption at 25°C .

On the contrary, the NO_x reactivity is much higher towards the hydrated substrates as reflected by the spectra reported in Figure 3.4.

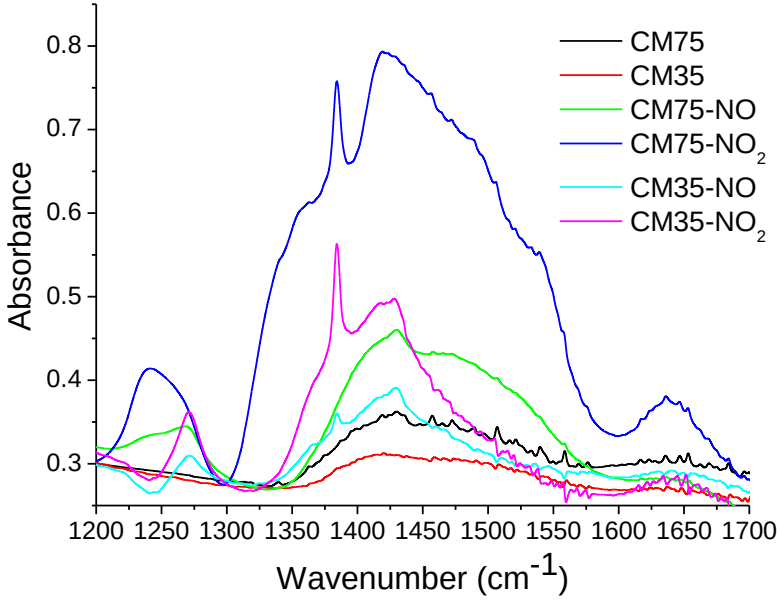

Figure 3.4 FTIR spectra of hydrated CaO/Mayenite substrates after NO and NO_2 adsorption at 25°C.

Thanks to the high intensity of the signal, the typical bands for nitrite (1271 cm^{-1}) and nitrates (1385, 1430, 1638 cm^{-1}) can be easily identified after exposure to NO or NO_2. The presence of water helps the nitrite formation also when the material is exposed to NO_2 because it promotes the NO_2 hydrolysis to yield NO_2^- and NO_3^-, that will be successively sorbed by $Ca(OH)_2$. In details, the surface reaction between NO_2 and $Ca(OH)_2$ generates nitrates through the formation of an OH radical intermediate and the successive reaction with NO[7]. The nitrites also come from the reaction of CaO –

$Ca(OH)_2$ with NO. After NO sorption a paramagnetic species, NO_3^{2-}, is formed and the reaction of NO_3^{2-} with $NO_{(g)}$ leads to the formation of more stable and diamagnetic species, such as the nitrite[8]. After a prolonged exposure the nitrites are converted to nitrate[9] and this reaction is at the base of the nitrate signals detected after the exposure of CaO/Mayenite substrates to NO.

Dehydrated PM exposed to NO and NO_2 does not show significant signals referred to nitrite and nitrate species, while nitrite species (1271 cm^{-1}) is detected after NO sorption on hydrated PM, moreover nitrite (1271 cm^{-1}) and nitrate (1385 cm^{-1}) are detected after NO_2 sorption (Figure 3.5).

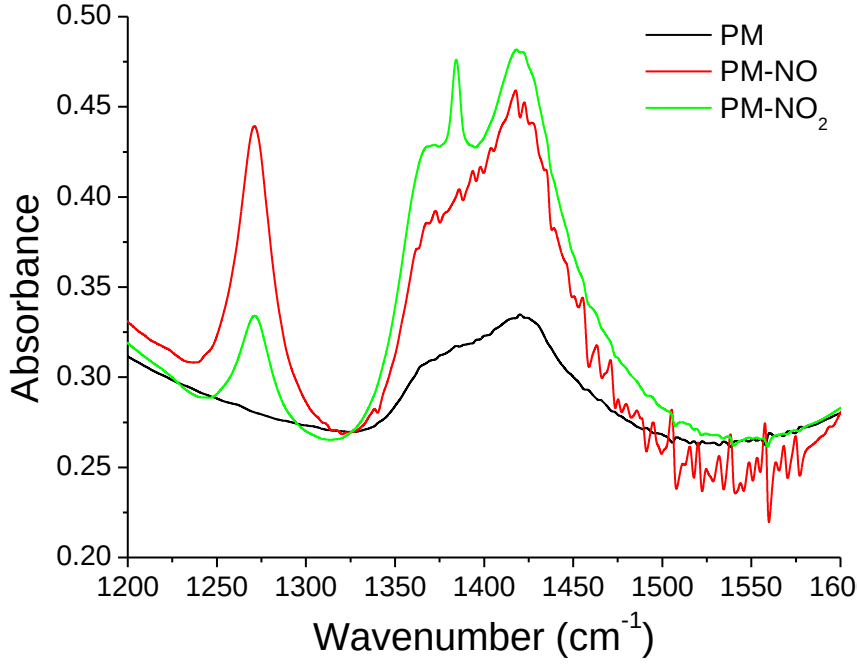

Figure 3.5 FTIR spectra of hydrated $Ca_{12}Al_{14}O_{33}$ after NO and NO_2 adsorption at 25°C.

Water favors NO_x capture on mayenite by surface sorption, similarly to what is reported for the calcium carbonate synthesis by the reaction between calcium hydroxide and carbon dioxide[10].

3.1.6 Ion chromatographic quantification of NO_x

In order to quantify the NO_x amount absorbed, 150.0 mg of each sample were extracted with 6.0 mL of 1.8 mM Na_2CO_3:1.6 mM $NaHCO_3$ solutions for 30 minutes at room temperature. NO and NO_2 were determined as nitrite and nitrate, after extraction, using a Dionex DX 120 ion chromatograph (Dionex, Sunnyvale, CA, USA), equipped with a Ion Pac AS14 column (4 mm × 250 mm). The eluent was 1.8 mM Na_2CO_3:1.6 mM $NaHCO_3$ at a flow rate of 1.1 mL min^{-1} and a pressure of 1350 psi. The calibration was performed by injecting 30 µl of four standard NO_2^- / NO_3^- solutions in the range 1.0 – 100.0 µg/mL. All the reagents were analytical grade. Chromatographic analyses were repeated three times in order to test the reproducibility of the instrument. For each type of sample (CM75, CM35, PM and the corresponding hydrated species) a set of three unexposed samples were analyzed to determine the blank values. According to EN 13528-2 the limit of detection (LOD) is expressed as three times the standard deviation of the blank values. Precision is estimated from 2σ deviation of the absolute differences of the individual sample values to the mean of the triplicate samples. Replicate precision was evaluated to be 0.4 % of the mean in all cases. Mean blank

levels (in μg) and LOD are listed in Table 4.1.

Table 3.1 Chromatographic analyses of freshly prepared sorbent materials (nitrates blanks and LOD).

Sample	NO_2^- (μg)	LOD (μg/mL)	NO_2^-	NO_3^- (μg)	LOD (μg/mL)	NO_3^-
CM75	0,003	0,0006		0,187	0,002	
CM75 hydrated	0,005			1,819		
CM35	4,582			20,56		
CM35hydrated	38,98			125,9		
PM	0,827			1,942		
PM hydrated	0,078			1,357		

Both the dehydrated and the hydrated CM35 show significant amounts of nitrite and nitrate as impurities of the synthetic process. The reaction mechanisms postulated from the FTIR spectra were confirmed by the quantitative determination of nitrites and nitrates through the IC analysis. After the exposure to NO_x, samples were extracted with a CO_3^{2-}/HCO_3^- buffer solvent and directly analyzed. The results in Table 3.2 and Table 3.3 show that the exposure of the PM, CM75 and CM35 to NO mostly results in the formation of nitrites, while nitrates are formed after nitrite conversion at longer period of exposure.

Table 3.2 Chromatographic analyses of Mayenite exposed to NO_x.

Sample	NO_2^- (µg)	NO_3^-(µg)
PM-NO	7,3	1,1
PM-NO_2	58,84	42,11
PM hydrated-NO	1154,09	<LOD
PM hydrated-NO_2	508,89	199,54

Table 3.3 Chromatographic analyses of CaO/Mayenite exposed to NO.

Sample	NO_2^- (µg)	NO_3^-(µg)
CM75-NO	711,22	89,12
CM75-NO_2	5,88	897,33
CM75 hydrated - NO	842,89	10,16
CM75 hydrated - NO_2	1694,41	7744,11
CM35-NO	368,11	111,75
CM35-NO_2	169,74	159,98
CM35 hydrated - NO	594,44	82,43
CM35 hydrated - NO_2	624,91	506,3

After NO_2 sorption, both nitrite and nitrate species are detected because the predominant reaction is the nitrogen dioxide hydrolysis on substrate surfaces followed by the reaction with CaO and $Ca(OH)_2$. The same reaction sequence is valid for PM. IC data also confirm an enhanced uptake of NO_x due to the hydration of the substrates and to the higher percentage of CaO in the materials.

Moreover, a new synthetic strategy have been developed to

favor the reduction of the blank values, crucial for any quantitative application. Mayenite was prepared using an hydrothermal method. 20.0 g of $Ca(OH)_2$ and 21.8 g of $Al(OH)_3$ were mixed in 0.8 L of distilled water and 200 mL of 2-propanol. This solution was stirred for 4 hour at room temperature and successively dried at 150°C for 8 hours, the solid was then calcined at 1000°C for 4 hours in the air to obtain a fine and porous powder. Following this procedure 26.0 g of pure mayenite were obtained. Chromatographic analysis performed after mayenite extraction as previously described shows nitrite and nitrate contents below the LOD.

3.1.7 Passive device preparation and preliminary field evaluation

Passive sampling devices (RING, Aquaria Research s.r.l.) were used to evaluate CO_2–NO_x exchange reactions. The diffusive body of the passive sampler is a micro-porous sintered polyethylene cylindrical tube. The internal concentric steel cartridge was filled with 500.0 mg of hydrated CM75 or CM35 after the total conversion of $Ca(OH)_2$ into $CaCO_3$.

Figure 3.6 RING passive sampler (Aquaria Research srl).

Carbonation reaction occurred in a sealed glass tube where substrates were saturated with a CO_2 flow (99.995% purity, Rivoira spa). Passive devices were placed in a rural area of South Italy for one week. Average temperatures were measured by a thermometer data-logger with ±1.0 °C accuracy. NO_x concentration in the atmosphere was monitored with an APNA-370 NO_x (Horiba) ambient monitor equipped with a chemiluminescent detector.

Results proved that CaO/mayenite materials could be successfully employed as sorbent substrates for NO_x in the atmosphere, depending on their hydration and on their CaO content. These characteristics allow to foresee an employment of CaO/mayenites substrate as field samplers or, on a larger scale, as remediation devices. A preliminary have been performed in a rural area of the South of Italy for one week, where passive sampling devices were loaded with CM75 and placed. Passive samplers are useful and cost-effective alternatives to conventional pumped samplers in

environmental monitoring when the average, instead of the real time, pollutant concentration is the object of the monitoring[11,12]. The most employed device for the monitoring of NO_2 is the TEA (triethanolamine) based passive sampler, which, however, presents one main drawback consisting in its freezing point (17.9 – 21.2 °C) that could lead to reduce NO_2 uptake at lower temperature. Moreover, TEA is a selective absorbent for NO_2 and cannot be used for NO_x (NO + NO_2) simultaneous measurements in air[13]. CM75 is a ceramic-type material and its performance are not significantly influenced by temperature changes and its affinity with both NO and NO_2 has been previously shown. The main purpose of the field test was to evaluate the potential interference of carbon dioxide on the sampling process. In fact, hydrated CaO/Mayenite substrates easily react with CO_2 to form $CaCO_3$ (no reaction occurs with dry substances)[3] and this competing reaction could affect the NO_x uptaking process in field experiments, where [CO_2] is much higher than [NO_x][14]. In the hydrated materials, the most important step of the reaction between CaO/mayenite and CO_2, is the carbonation of $Ca(OH)_2$[10,15] according to the following reaction:

$$Ca(OH)_{2(aq)} + CO_2 \longrightarrow CaCO_{3(s)} + H_2O_{(l)}$$

wherein the formation of calcium carbonate is most probably preceded by the formation of calcium carbonate hydroxide hydrate and calcium carbonate hydrate[14,16]. Rendek et al.[17] stated that the CO_2 dissolution and diffusion in the water layer is the rate-limiting step of the carbonation reaction; moreover, they found that an increase of the CO_2 concentration in the aqueous phase accelerates the reaction without any change in the amount of formed carbonates.

In order to evaluate the competing sorption of CO_2 on the NO_x uptake process, we used passive sampling devices loaded with pre-carbonated substrate. The formation of $CaCO_3$ according to the reaction previously described, augments the sample mass proportionally to the amount of trapped CO_2, therefore thermo-gravimetric analysis (TGA) in a nitrogen atmosphere, has been used to evaluate the chemical composition of $CaCO_3$/Mayenite substrates after NO_x sorption in the environment. In particular, the amount of the captured CO_2 has been measured from the weight loss during the heating phase between 500 °C and 800 °C in the furnace[16,18]. Figure 3.6 shows the TGA thermogram of a hydrated sample of CM75 pre-carbonated in the laboratory by using a standard Schlenk technique. In this pilot experiment, the captured CO_2 mass was 165 mg per 1 g of substrate, corresponding to a

mass loss of 16.5%.

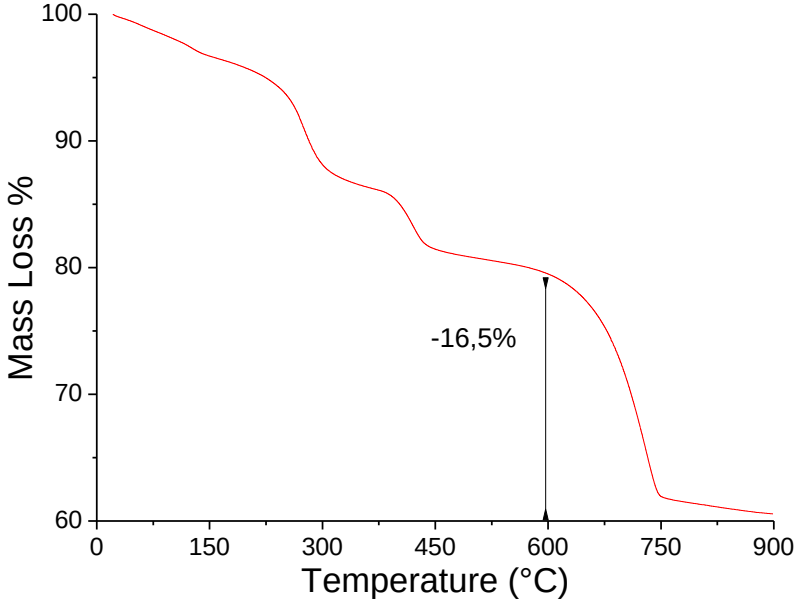

Figure 3.7 Thermogram of carbonated substrate.

For the field experiments, 500.0 mg of pre-carbonated and not pre-carbonated CM75 were injected into different RING passive sampler and afterward placed in sampling sites, where an atmospheric NO_x concentration of 0.06 ppm (averaged over one week) was measured by means of a NO_x analyzer as the sum of NO and NO_2. After the sampling period, thermograms of the substrates showed a mass loss related to decarbonation reaction of 16.3%, confirming that pre-carbonated CM75 does not further react with CO_2 and not pre-

carbonated CM75 sorbes the same amount of CO_2 as in the laboratory tests. The NO_x uptake was evaluated by IC analysis and both nitrites and nitrates were found. According to previous results[19] the reaction mechanism in the presence of CO_2 can be outlined as follows:

$$Ca(OH)_2 + CO_2 \longrightarrow CaCO_3 + H_2O \quad (3)$$

$$NO + 1/2O_2 \longrightarrow NO_2 \quad (4)$$

$$Ca(OH)_2 + 3NO_2 \longrightarrow Ca(NO_3)_2 + NO + H_2O \quad (5)$$

$$CaCO_3 + 3NO_2 \longrightarrow Ca(NO_3)_2 + NO + CO_2 \quad (6)$$

the $CaCO_3$ formed can react with NO or NO_2 to form $Ca(NO_3)_2$ as shown in reaction 5. NO released in reactions 5 and 6 can react again with O_2 to form NO_2 according to reaction 4 so that reactions 5 and 6 occur repeatedly to form again NO[19]. Data from IC analyses reported in Table 3.4 show that the competition with CO_2 does not significantly affect the sorption capacity of the CaO/mayenite substrates towards the atmospheric NO_x.

Table 3.4 Chromatographic analyses of CM75 in field experiments.

Sample	**NO_x (µg) as NO_2^- + NO_3^-**
CM75 (pre-carbonated) raw material	0,028
CM75 (not pre-carbonated) afetr sampling	2,600
CM75 (pre-carbonated) after sampling	2,734

In fact after one week of exposure, the not pre-carbonated substrates convert the same amount of NO_x, measured as the sum of nitrates and nitrites, as the pre-carbonated CM75.

3.1.8 Conclusions

A new class of convenient and effective substrates exploitable for environmental applications have been investigated. Three different Ca-based NO_x sorbents (CM75, CM35 and PM) were synthetized and characterized, either by the integration of CaO with the metal oxide $Ca_{12}Al_{14}O_{33}$ or by a sol-gel synthesis from raw materials. FTIR and IC analysis showed a good capacity of NO and NO_2 sorption, which took place mainly through the formation of nitrates and nitrites species on the sorption surface. The NO_x uptake was found to be dependent both on the hydration degree and on the percentage of CaO of the materials since water and calcium hydroxide play a fundamental role for the NO_x capture mechanism. Finally, carbon dioxide interference was investigated in order to evaluate a possible use of Ca-based substrates as NO_x sorbent in radial diffusive sampler for atmospheric monitoring and remediation and it was found that CO_2 does not influence significantly the NO_x uptake. Future studies are necessary to define the passive sampling rate for NO_x in order to characterize in detail the passive sampler and to give the opportunity to measure the NO_x concentration in the atmosphere.

References

(1) Z. Li et al., *Energy Fuels* **2005**,19,1447-1452
(2) M. F. Zawrah et al., *Ceram. Int.* **2007**,33,1419-1425
(3) R. Cucciniello et al., *Atmos. Environ.* **2012**,60,82-87
(4) M. G. Suryaraman et al., *J. Chem. Educ.* **1949**,26,594
(5) G. I. Zhmoidin et al., *Cem. Concr. Res.* **1984**,14,386-396
(6) C. Li et al., *Mater. Res. Bul.* **2011**,46,1307-1310
(7) G. Chen et al., *Ind. Eng. Chem. Res.* **2010**,49,1450-1456
(8) M. Paganini et al., *J. Phys. Chem. B* **2002**,106,12531-12536
(9) C. Verrier et al., *Catal. Today* **2008**, 136,121-127
(10) J. Meima et al., *App. Geochem.* **1999**, 14,159-171
(11) R. H. Brown, *J. Environ. Monit.* **2000**,2,1-9
(12) T. Gorecki et al., *Trac Trends Anal. Chem.* **2002**,21,276-291
(13) C. Kirby et al., *J. Environ. Monit.* **2000**,2,307-312
(14) A. Kalinkin et al., *Inorg. Mater.* **2005**,41,1073-1079
(15) A. C. Garrabants, *Rutgers University*, **2001**,396
(16) E. T. Stepkowska et al., *J. Therm. Anal. Calor.* **2007**,87,189-198
(17) E. Rendek et al., *J. Hazard. Mater.* **2006**,128,73-79
(18) S. Mojumdar et al.,*J. Therm. Anal. Calor.* **2006**,83,135-139
(19) N. Matsushima et al., Envi. Sci. Tech. 2004,38,6867-6874

3.2 CO_2 sorption on $CaO/Ca_{12}Al_{14}O_{33}$ substrate for carbon isotope ratio analysis

3.2.1 CO_2 sorbent material preparation

Calcium oxide based sorbent was prepared by following the procedure proposed by Li et al.[1], as follows: 56.8 g of aluminium nitrate enneahydrate [$Al(NO_3)3 \cdot 9H_2O$] and 52.4 g of calcium oxide were added into a mixture of distilled water (1.5 L) and 2-propanol (260 mL) so that the weight ratio of calcium oxide to the newly formed mayenite ($Ca_{12}Al_{14}O_{33}$) would become 75:25 w/w. This solution was stirred for 1 h at 75°C and successively dried at 120°C for 18 h before being roasted at 500°C for 3 h in the air. This method produced a fine and porous powder. After calcination, distilled water was added to the mixture and the obtained paste was dried at 120°C for 2 h and then calcined in air at 800°C for 1.5 h. Before exposure to CO_2, the sorbent was "activated" by hydrating with water vapour in a closed system for seven days. Hydration was also necessary to avoid interferences due to variable atmospheric humidity during the exposition, and to avoid potential errors in the quantitative evaluation of trapped CO_2[2].

3.2.2 $CaO/Ca_{12}Al_{14}O_{33}$ characterization

The quantitative determination of the captured CO_2 can be performed by TGA by evaluating the weight loss in the furnace during heating. Loss in sample weight between 500 °C and 800 °C in an inert atmosphere, is directly correlated to the carbonate content of the sorbent, and hence to trapped carbon dioxide[3,4]. The mass sample evolution was recorded, as a function of temperature, by using a Netzsch TG 209 apparatus.

In the past, several absorbents have been used for passive CO_2 samplers including hydroxides and molecular sieve for collecting samples for $^{14}CO_2$ analysis[5] while no work in the literature reported the passive sampling approach for collecting samples for $\delta^{13}C$ analysis. Cooper et al.[6] provided one example of passive sampling for $^{14}CO_2$ measurement using hydroxides while Davidson[7] noted that hydroxide, since even fresh, may contain a significant quantity of CO_2 that could lead to sample contamination.

Additionally, hydroxides are potentially harmful, requiring care during deployment. Ca-based sorbent, used this study, does not show carbon dioxide impurities after synthesis due to the high temperature of the synthetic process. Moreover, in order to avoid contamination, $CaO/Ca_{12}Al_{14}O_{33}$ 75:25 w/w

substrates were kept under inert atmosphere before exposure. Fresh Ca-based sorbent material did not show any significant presence of CO_2.

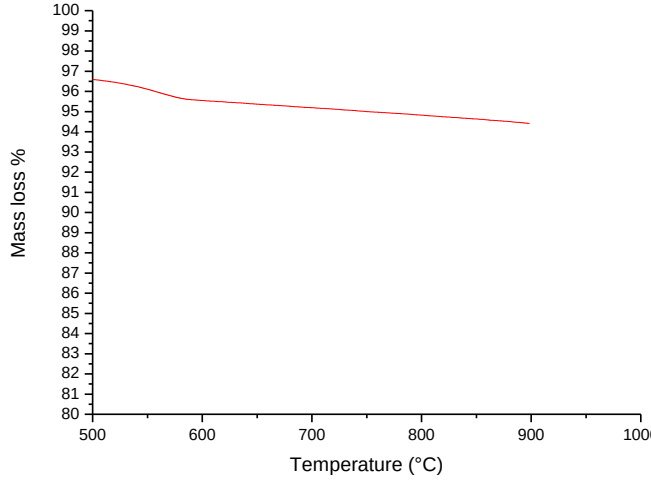

Figure 3.8 Thermogram of fresh $CaO/Ca_{12}Al_{14}O_{33}$ sorbent.

3.2.3 Field measurements

$\delta^{13}C$ measurements was performed over a period of seventeen months, from November 2011 to April 2013, in three different environments in order to investigate spatial variations and a possible correlation with carbon dioxide concentration in air. The tested sites were a commercial area, a rural area and a common kitchen in a private house. An elevated density of traffic and population characterized the commercial area,

while the two other sites were selected based on their different carbon dioxide emission sources. The rural area was far away from manmade sources of CO_2 pollution while the major emission source in the private kitchen was the natural gas combustion.

Carbon dioxide for $\delta^{13}C$ measurements was collected by means of diffusive sampling technique. The diffusive body was the commercial RING from Aquaria Research Srl, where the internal concentric steel cartridge was filled with 500.0 mg of a $CaO/Ca_{12}Al_{14}O_{33}$ 75/25 w/w hydrated sorbent. The exposure time for CO_2 capture was fixed in 3 days in order to obtain an adequate amount of analyte for carbon isotope ratio analysis, 20 mg being the minimum required. Figure 4.9 shows the loading trend of the CO_2 mass in the sampler towards the time of exposition.

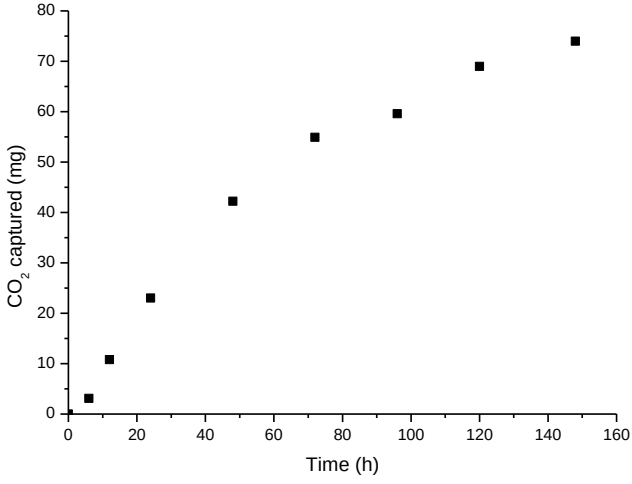

Figure 3.9 CO_2 mass uptake profile versus time.

The samplers were located at a height of 2 m above the street level in the urban and rural areas and at 1 m of height in the private kitchen. Three passive samplers were used for each determination and they were coupled with a portable Q-Trak Plus IAQ instrument for carbon dioxide determination in order to compare CO_2 concentration values obtained by passive and active devices.

3.2.3 Carbon isotope ratio analysis and evaluation of possible isotopic fractionation

Generally, the isotopic ratio is carried out by analysing carbon dioxide obtained by converting the carbon contained within a sample. Isotope ratio mass spectrometry (IRMS) is the standard technique used for highly accurate $\delta^{13}C$ determinations. However in the past[8] it has been showed that $^{13}C/^{12}C$ carbon isotope ratio, can be simply obtained by means of inexpensive FT-IR spectroscopy of carbon dioxide trapped within a polymer according to an easy and fast protocol. The reliability of the method was assessed in a study dedicated to the ^{13}C - urea breath test in the non-invasive diagnosis of helicobacter pylori infection[9], where authors found a good correlation between FT-IR spectroscopy and the established one.

$\delta^{13}C$ analysis was conducted by means of a HeliFANplus analyzer equipped with a single beam non-dispersive infrared industrial photometer. After the exposure at the sampling locations, the sorbent materials were placed into a glass flask and mixed with 2.5 ml of orthophosphoric acid to develop CO_2 from the carbonates. CO_2 was then gathered into the aluminized breath bags connected with the inlet ports of the NDIR spectrometer for sequential measurements. The NDIR

device was connected to a computer, which enables the software-guided measurement and calculation of results. Three samples were analyzed for each determination.

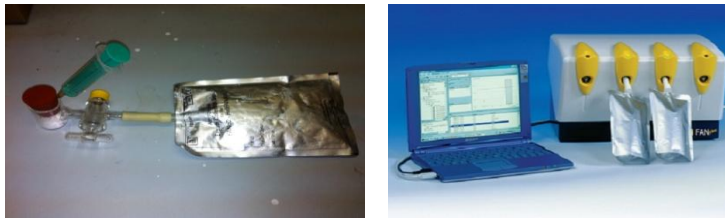

Figure 3.10 Experimental set-up

A pilot study was conducted in laboratory to determine whether passive sampling caused isotopic fractionation. Each sampler (used in triplicate) was held for 45, 90, 150 and 180 minutes in a bottom flask connected with a tube to a CO_2 cylinder (99,995% purity, Rivoira spa). The $\delta^{13}C$ of passive samples were compared with those obtained using an evacuated flask wherein carbon dioxide was collected directly into the breath bags.

Passive samplers were exposed for 3 days in three different environments to capture atmospheric CO_2 and evaluate differences in the isotopic composition. Moreover air samples were concurrently collected using a pump-based system in order to compare the results of CO_2 concentration obtained both by passive and active devices. In Figure 3.11 the isotopic domains of the different areas investigated are reported.

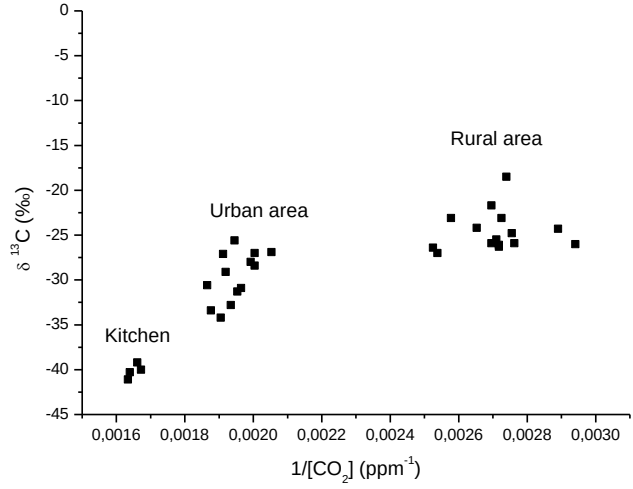

Figure 3.11 $\delta^{13}C$ versus $1/[CO_2]$ concentration diagram (Keeling plot) of the different areas investigated.

It can be easily observed that the CO_2 recovered from the passive samplers had an isotopic composition representative of the atmosphere being sampled. In fact for the rural area, where the contribution to CO_2 is essentially that of the respiring process of plants and soil we can observe a domain characterized by a low level of CO_2 (concentration ranging between 340 and 400 ppm) and $\delta^{13}C$ values ranging between -18,5‰ and -27‰, whereas for the urban environment we can see a higher concentration of CO_2 (387-562 ppm.) with a $\delta^{13}C$ varying from -25,6‰ to -35‰ deriving from various and different sources (mostly combustion process involving fossil

fuels). Finally for the civil inhabitation data were recorded in the proximity of the kitchen and they are consistent with the burning of methane and other hydrocarbons ($\delta^{13}C$ varying from -40‰ to -45‰, with an average value of CO_2 equal to 600 ppm). In the urban area monitored the major source of carbon dioxide is the vehicular traffic. Thus, with the aim to compare results of isotopic composition of atmospheric CO_2 and the vehicle gas emission, vehicle exhaust gas was sampled choosing two different auto vehicles running on unleaded gas and diesel fuel purchased from distributor of the test area. Prior to each sampling vehicles were idled for 10 min to reach operating temperatures[10]. The aluminized breath bag was directly connected by means of a glass funnel to the exhaust pipe in order to collect the exhaust gas, than connected with the inlet ports of the NDIR spectrometer for measurements. Five measurements were performed for each vehicle exhaust gas and the results, which are in agreement with those reported in Figure 3.11 for the urban area, are shown in table 3.5.

Table 3.5 Isotopic compositions of exhaust collected from various vehicles.

Supply system	**$\delta^{13}C$ (‰)**
Unleaded petrol	-27.5±0.6
Diesel fuel	-32.9±0.4

In the field experiments, atmospheric concentration of CO_2 and isotopic ratios vary temporally, making it difficult to determine whether rates of collection are proportional to the CO_2 concentration and to precisely quantify any isotopic fractionation, which might occurs. This possibility was ruled out by carrying out a laboratory experiment in which passive samplers were used inside a 30L airtight plastic barrel and they were exposed to a constant CO_2 flux for different time.

Data collected were identical for each measurement, within the technique precision, and comparable to those concurrently obtained by directly collecting CO_2 into the breath bags, thus demonstrating that there was not isotopic fractionation caused by the $CaO/Ca_{12}Al_{14}O_{33}$ 75:25 w/w hydrated substrate.

Moreover, as it was already done in a previous work in order to assess the accuracy of passive measurements[(2)], concentration of CO_2 was concurrently measured by the passive device and with a portable active sampler (Q-Trak

Plus IAQ). The comparison of the passive sampler to the active reference method produced good results, in fact in all cases the values obtained by passive measurements (reported as average values of CO_2 concentration) fall in the range covered by continuous measuring (between the minimum and maximum value registered). A good correlation between the two techniques was evident, Pearson's correlation coefficient being 0.879 and all the model parameters significant at a 99% confidence level ($p < 0.001$).

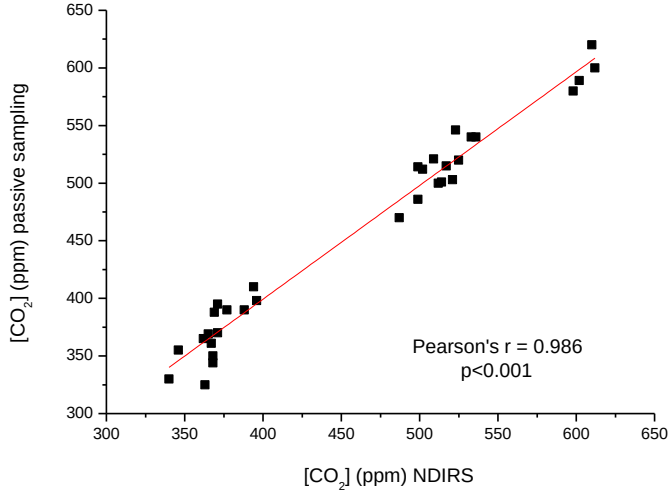

Figure 3.12 Correlation between values obtained by the passive devices and the NDIRS measurements.

3.2.5 Conclusions

Measurement of $\delta^{13}C$ in atmosphere was performed by using a Ca-based solid absorbent to passively collect CO_2. Ca-based absorbent ($CaO/Ca_{12}Al_{14}O_{33}$ 75:25 w/w) does not shows CO_2 impurities, as found in the past for hydroxide based substrate used for CO_2 capture, reducing possible interferences in the determination of $\delta^{13}C$, and does not show isotopic fractionation. Measurements were conducted in three different environments in order to exploit differences/similarities between both *indoor/outdoor* ambient. Three different domains of $\delta^{13}C$ vs. CO_2 concentration were found, indicating the different nature of the CO_2 in the investigated areas, as expected taking into account the capability of $\delta^{13}C$ to provide information on the source of this greenhouse gas. In this thesis it is described the first reliable example of a passive device for $\delta^{13}C$ determination in air for CO_2 source investigation, enhancing the choice of diffusive samplers for the evaluation of air quality.

References

(1) Z. Li et al., *Energy Fuels* **2005**,19,1447-1452
(2) R. Cucciniello et al., *Atmos. Environ.* **2012**,60,82-87
(3) S. Mojumdar et al.,*J. Therm. Anal. Calor.* **2006**,83,135-139
(4) E. T. Stepkowska et al., *J. Therm. Anal. Calor.* **2007**,87,189-198
(5) M. H. Garnett et al., *Atmos. Envir.* **2010**,44,877-883
(6) E.L. Cooper et al., *Appl. Radiat. Isot.* **1998**,49,1307-1311
(7) G.R. Davidson, *Geoch. Cosm. Acta* **1995**,59,2485-2489
(8) R. Zanasi et al., *Anal. Chem.* **2006**,78,3080-3083
(9) O. Motta et al., *J. Infec.* **2009**,59,90-94
(10) N. Turner et al., *Atmos. Environ.* **2006**,40,3381-3388

3.3 Use of mayenite as active supports in catalysis

3.3.1 Preparation of mayenite based catalysts

Mesoporous mayenite was prepared by sol-gel synthesis as shown in Chapter 3.1. The starting material for the sol-gel process included calcium nitrate tetra hydrate [$Ca(NO_3)_2$*$4H_2O$], aluminium nitrate enneahydrate [$Al(NO_3)_3 \cdot 9H_2O$] and citric acid ($C_6H_8O_7$) as organic fuel. 69,6 g of calcium nitrate and 111,6 g of aluminium nitrate were added to 1,5 L of distilled water. The mixture was heated on a hot plate at 60°C, than 5 g of citric acid was added. The citrate-nitrate mixture was heated and vigorously stirred with magnetic agitator at 90°C until a gel was formed, about 12 hours.

The resulting gel was placed in a drying oven at 130°C where auto-combustion occurs and the gel transformed into a cake-like structure, which was subsequently crushed into powder using the agate mortar and pestle. The resulting powders were fired into a furnace at 1000°C in air for 4 hours. 26.0 g of mayenite were obtained using this synthetic methodologies.

Palladium loaded mayenite was prepared by reduction of $PdCl_2$ with $NaBH_4$ in a THF solution. 0.0895 g of $PdCl_2$ and 4.9481 g of mayenite were added to 250 mL of distilled water. The mixture was stirred for 4 h at room temperature than the

solid was filtered, dried at 120°C for 20 h and was added to a 0.1 M solution of $NaBH_4$ in anhydrous THF. The mixture was stirred for 5 h than the catalyst was recovered by filtration, washed with hot distilled water and dried at 250°C for 16 h and calcined at 800°C for 4 h. A commercial 10% Pd/C catalyst was also used for comparison.

3.3.2 Catalysts characterization

X-ray diffraction patterns were obtained on a Bruker D8 Advance automatic diffractometer operating with a nickel-filtered CuKα radiation. Data were recorded in the 2θ range of 4-80° with the resolution of 0,02°.

XRD studies were carried out for (A) 1% wt Pd/mayenite and (B) mayenite as shown in Figure 3.13. Since the metal loading was very low no characteristic peak for Pd (111) was obtained at 2θ = 40°. Mayenite shows its characteristic crystalline structure after metal loading procedure.

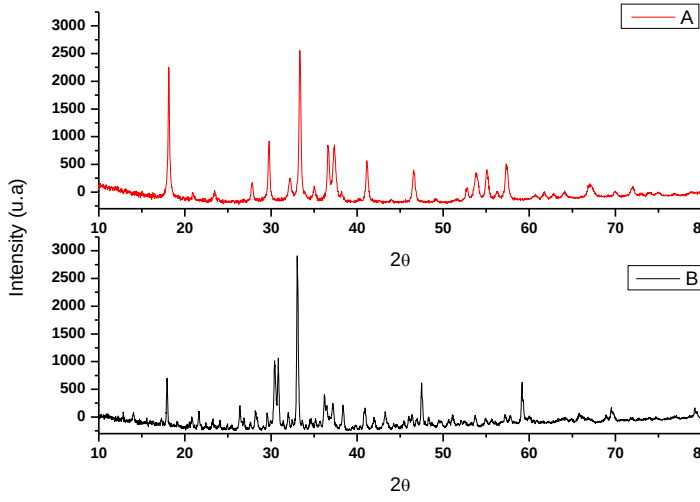

Figure 3.13 XRD pattern of (A) 1% wt Pd/Mayenite and (B) pure mayenite.

The BET surface area of catalysts were determined using a Nova Quantachrome 4200e instrument using nitrogen as the probe molecule at liquid nitrogen temperature (-196°C). Before the adsorption measurement, Pd/C catalyst was degassed at 40°C under vacuum for 24 h, while mayenite was degassed at 200°C for 12 h in the same conditions. The surface area values were determined by using 11-point BET analysis. Catalyst pore size distribution was derived from pore volume of the nitrogen desorption branch.

Palladium content in mayenite was determined by ICP-OES analysis by digesting the sample in aqua regia (37% HCl and

70% HNO_3 3:1 ratio). The metal loading found out was 1,09% for Pd/Mayenite.

BET surface areas of mayenite based materials and commercial Pd/C catalyst are shown in Table 4.5. An unexpected increase in the surface area of mayenite after Pd loading was observed (from 5.4 to 16.9 m^2/g). Actually the loading of a metal on a substrate results commonly in a reduction of the surface area due to the filling of the pores by the metal particles[(1)]. In this case such increase is probably due to the milling of the substrate during the catalyst preparation process involving continuous stirring. For comparison, the surface area of commercial Pd/C catalyst was also measured, that was found to be 770 m^2/g.

Table 3.5 BET surface area analysis.

Material	**Surface area, m^2/g**
Mayenite	5,4
1% Pd/Mayenite	16,9
10% Pd/C	770

The adsorption-desorption isotherms of nitrogen for mayenite is shown in Figure 4.14 and according to the IUPAC classification, the N_2 isotherm is of type IV characteristic of

mesoporous materials[2]. The BJH pore size distribution show pore volume of 0.01 cm^3/g while the average diameter of holes is 11.4 nm. Palladium loaded mayenite preserves characteristic of mesoporous material, while commercial Pd/C catalyst is classified as microporous.

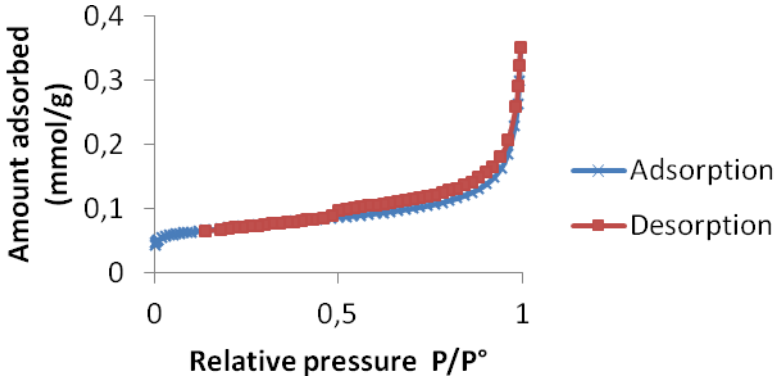

Figure 3.14 N_2 adsorption-desorption isotherm of mayenite.

The morphological and elemental analysis have been performed by a scanning electron microscope (SEM, Tescan Vega LMU) equipped with a X-Ray energy dispersive microanalysis of elements having an atomic number >4, with a resolution of MnKα less than 123 eV (100.000 cps) (EDX, Bruker Quantax 800). SEM images have been obtained by secondary electrons (SE) with an accelerating voltage of 25,00 KV. The EDX spectra were obtained with an

accelerating voltage of 25,00 KV and with a WD of 15,0 mm. X-Ray intensities were converted in wt% elements by a standardless ZAF quantification.

SEM images in Fig. 3.15 A show that mayenite is characterized by the presence of sheets and two types of pores can be observed: large macropores on the μm scale (see the left column of Fig.3.15) and mesopores on the nm scale (see the right column of Fig.3.15). From SEM images, it can be seen that the Pd/mayenite sample (Fig.3.15 B) still retains significant porosity, even if the sheets seem to be grown during the catalyst preparation. However, both macropores and mesopores can be still observed in Pd/mayenite sample.

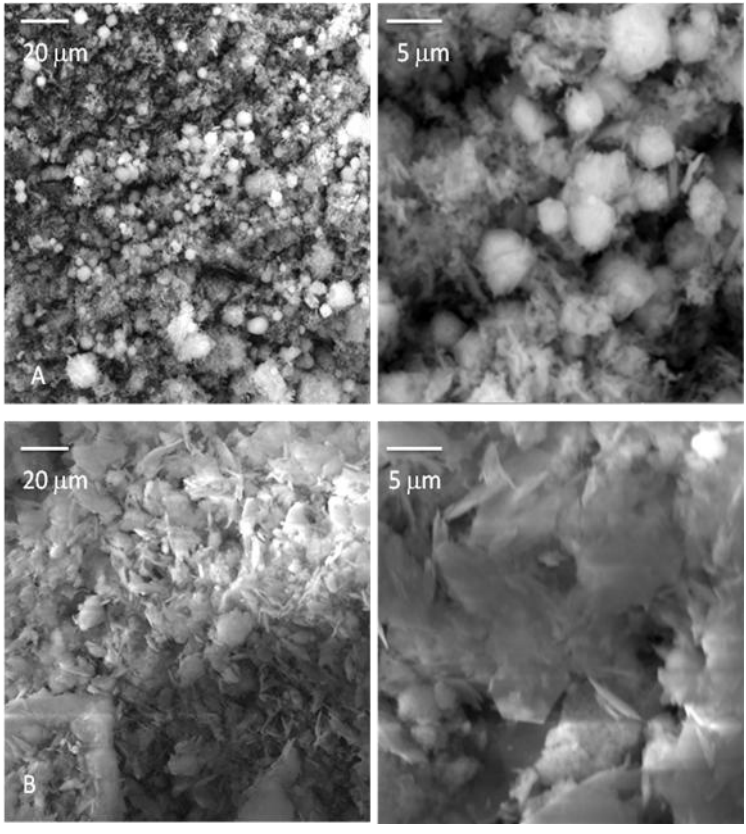

Figure 3.15 SEM images of (A) mayenite and (B) Pd/mayenite. Magnification: 2kx (left column), 10Kx (right column).

In Fig.3.16 reports the map of Pd distribution in the area shown in Fig.3.15 B at 10Kx. The intensity of the color is proportional to the Pd concentration and each pixel correspond to a spectrum. EDS analysis of the material shows that Pd is not uniformly distributed on mayenite, as it is clear in Fig.3.16. Moreover, two different regions are present. Region I consists mainly of Ca, Al and O (in which Ca and

Al are present in atomic ratio similar to that present in mayenite) and less amount of Pd and Cl (<1 wt%, atomic ratio Pd/Cl 0.51±0,09), as it is shown by the representative related spectrum in Fig.3.16 Region II is rich in Pd (18±4 wt%) while Cl is less than 1 wt% and the remaining amount is constituted by Ca, Al and O in atomic ratios similar to those present in mayenite (spectrum in Fig.3.16). Region I is essentially characterized by the original recrystallized mayenite with trace of not reacted $PdCl_2$ and even if elemental Pd is present it is very low and it is under the experimental uncertainty of the technique. Instead, region II presents palladium loaded mayenite.

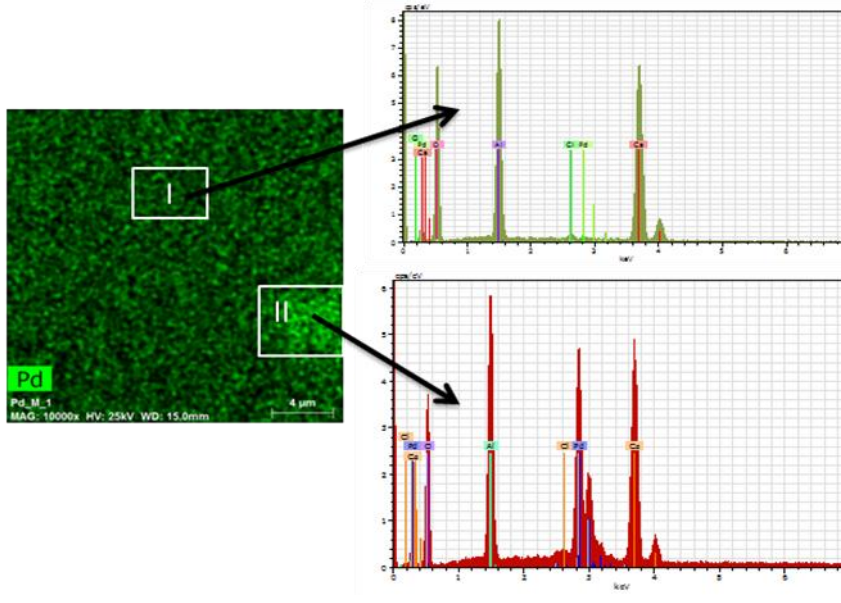

Figure 3.16 Map of Pd distribution in the area shown in figure 3.15 at 10Kx and EDS spectra of the regions I and II in the dotted areas.

The transmission electron microscopy (TEM) images were obtained by using a Jeol Jem 1011 microscope (Jeol, Tokyo, Japan) operating at an accelerating voltage of 100 kV. The samples were prepared by dropping mayenite diluted solution in ethanol onto 400-mesh carbon coated copper grids and evaporating the solvent. TEM micrographs were also taken to show Pd particles into the mayenite structure. Picture show that palladium particles were in the nano range but not well dispersed (Fig.3.17).

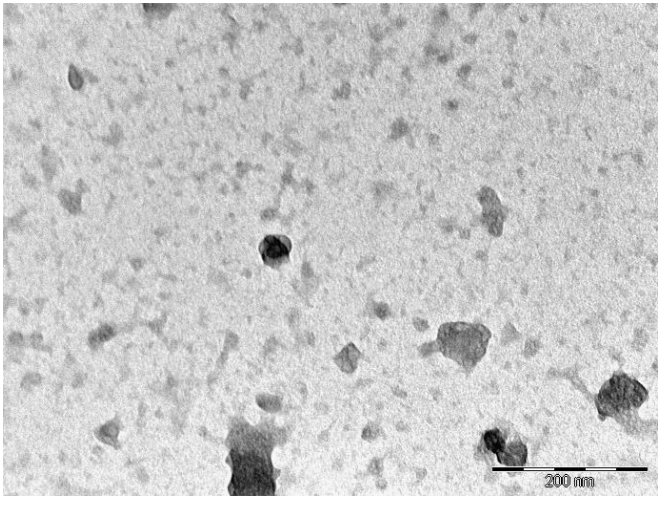

Figure 3.17 Transmission electron micrograph of 1% wt Pd/Mayenite.

3.3.3 Hydrogen sorption experiments

Hydrogen adsorption isotherm at 25°C over the range 1-15 bar were obtained using a Quantachrome I-Sorb HP using ultra pure 6.0 grade H_2 (99.9999%V; Rivoira). Prior to the measurements, samples were degassed at 200°C for 48 h. Analysis were conducted on 0.5 g of sample. Hydride characterization was made by ^{1}H-NMR magic angle spinning nuclear magnetic resonance spectra measured with a Bruker Avance 300 spectrometer. The rotation frequency was 15 kHz. Experiment was conducted on ca. 0.1g of powdered sample. Chemical shift scales were calibrated with the methylene absorption of the adamantine standard. Figure 4.18 illustrates the hydrogen sorption isotherms of mayenite collected at 25°C. The maximum amount of hydrogen sorbed as hydride results $2.4*10^{18}$ cm^{-3}, considering a mayenite density of 2.85 g/cm^3. This value is two orders lower than that reported by Hayashi[3] of $2.5*10^{20}$ cm^{-3} obtained after hydrogen sorption on mayenite at 1300°C because, as expected, temperature plays an important role on the dissociation of hydrogen molecules. Hydrogen is sorbed as hydride and this mechanism is different from H_2 adsorption on charcoal adsorbent where the gas molecules are undissociated. As reported in literature[4], porous carbon

materials, thanks to their high surface area values, show good performances for hydrogen storage applications with a significant uptake capacity of 0.23 wt% / 1000 m^2/g of carbon sorbent at 25°C and 100 atm. This value is greater than three order of magnitude of that obtained with mayenite.

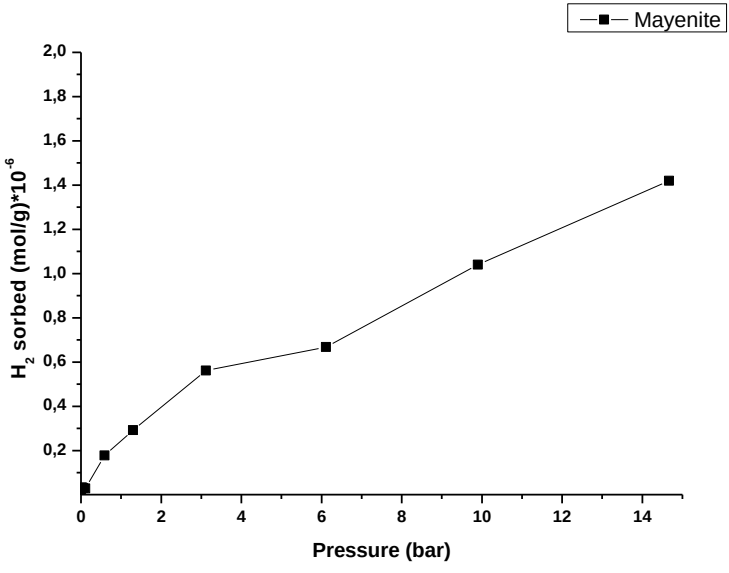

Figure 3.18 Hydrogen sorption profile of mayenite at 25°C.

Hydride ions incorporated into the cages of mayenite after H_2 adsorption at 25°C for 48 h have been characterized by ^{1}H-MAS NMR. The signal at 4.9 ppm (Fig.3.19) is assigned to the H^- ions in cages according to literature[5].

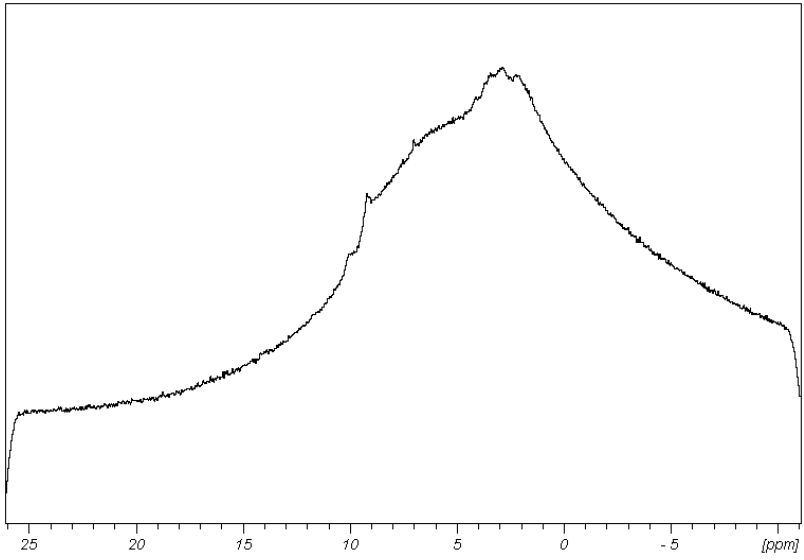

Figure 3.19 ^{1}H-NMR of mayenite hydride.

3.3.4 Aldehydes hydrogenation reactions

Benzaldehyde hydrogenation using solely mayenite was carried out in a high-pressure reactor of 150 mL capacity equipped with a pressure gauge, safety valve, valves for gas inlet and outlet and a thermocouple for temperature sensing. 0.5 g of mayenite and 5 mL of benzaldehyde (>99%, Sigma Aldrich) were added into a glass vial equipped with a magnetic stirrer. The reactor was charged with pure hydrogen (>99%, Rivoira) at a pressure of 8 bar and maintained at 80°C. The reaction was carried out for different times (1 to 168 h) and samples were analyzed using GC-MS instrument

(Agilent 7890A) with HP-INNOWAX fused silica capillary column.

Aldehydes hydrogenation with metal loaded mayenite (Pd/Mayenite 1% wt) were conducted at 20 and 120°C at an hydrogen pressure of 8 bar in the range 1-24 h, using 10 mL of diethyl ether as solvent (>99.5%, Sigma Aldrich) and a substrate/metal ratio of 1000 (0.025g catalyst and 0.25mL benzaldehyde). For comparison reactions with Pd/C 10 % wt were conducted using the same substrate/metal ratio (0.025g catalyst and 2.5mL benzaldehyde) and reaction conditions.

Firstly, mayenite hydride reactivity was evaluated in the solvent free reduction of benzaldehyde, using high-pressure reactor.

Hydrogenation of benzaldehyde was carried out at 80°C under a pressure of 8 bar of hydrogen at different reaction times. The conversion increases with time upper to a value of 12% after one week with good selectivity (95% benzyl alchol).

Notwithstanding this result is not significant in term of conversion this behavior reveals an important aspect referred to the reactivity of the mayenite containing H^- ions. Remarkably, when benzaldehyde hydrogenation was carried out using 0.5 g of mayenite hydride (preformed through thermal treatment at 1300°C of mayenite under hydrogen

atmosphere 4 h, 8 bar H_2) and 0.5 mL of benzaldehyde dissolved in 10 mL of diethyl ether at 25°C for 3 days, without feeding hydrogen, benzyl alcohol was selectively formed with the same conversion of 12%. These results indicate that $6*10^{-4}$ mol of hydride were formed and such observation was in agreement with that found by Hayashi[6] in similar conditions. This behavior suggests that the reduction is most probably due to the hydride present in the mayenite pores rather than to the H_2 molecules of the feed. However the presence of hydrogen is fundamental in the case of mayenite directly obtained by sol-gel preparation because the hydride ions are formed during the course of the reaction.

In order to increase the conversion in the reduction reaction, the possibility to use mayenite as support for palladium in the hydrogenation reaction was explored comparing the results obtained in the presence of such non-innocent substrate to a well-known, commercially available, catalytic system such as palladium supported on charcoal (Pd/C). In order to evaluate the effect of temperature on conversion, the reactions were carried at 20 and 120 °C. The effect of temperature and the reaction time on the conversion of benzaldehyde to benzyl alcohol is shown in Fig. 3.20 and the results are reported in more detail in Table 3.6.

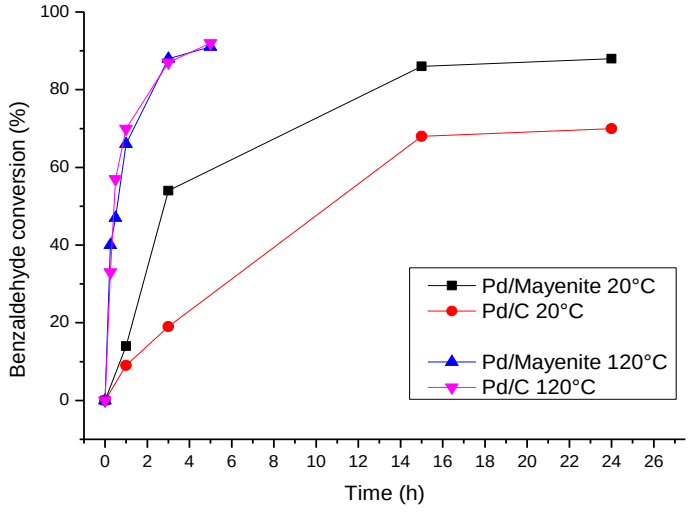

Figure 3.20 Benzaldehyde conversion using Pd/Mayenite and Pd/C as catalysts.

Table 3.6 Effect of time and temperature on benzaldehyde conversion.

	Time (h)	Pd/Mayenite	Selectivity	TOF (h^{-1})	Pd/C	Selectivity	TOF (h^{-1})
T= 20°C		Conversion %	Benzyl alcohol %		Conversion %	Benzyl alcohol %	
	1	14	>99	149.7	9	>99	95.6
	3	47	>99	166.6	19	>99	67.6
	15	66	>99	46.9	68	>99	48.4
	24	87	>99	38.8	70	>99	31.2
T=120°C	0,25	14	>99	598.3	33	88	1408.6
	0,5	54	>99	1156.5	57	86	1217.4
	1	66	>99	704.3	70	80	747.8
	3	88	>99	313.1	87	15	310.2
	5	91	>99	194,6	92	13	196.8

Reaction conditions for Pd/Mayenite catalyst: 0.025g catalyst, 0.25 mL benzaldehyde, 10 mL diethyl ether, 8 bar H_2.

One can observe that the conversion increases considerably with temperature giving only the 14% of conversion after 1 hour at 20°C and the 66% at 120°C respectively . Notably the selectivity towards benzyl alcohol is retained at high temperature using mayenite as substrate (100%). In the case of Pd/C catalyst increasing the temperature from 20 to 120 °C has an even stronger affect on the catalytic activity (after 1 h the conversion is 9% at 20 °C and 70% at 120 °C respectively) but the selectivity towards benzyl alcohol fall down from 100% at 20 °C to 13% at 120 °C. Indeed the analysis of the reaction mixture reveals the presence of benzyl ether as the only by-product. The formation of this compound instead of the desired benzyl alcohol is reasonably due to the presence of the acidic charcoal as substrate that can promote the etherification reaction of the formed benzyl alcohol[7]. Such reaction pathway is confirmed by the fact, that the formation of benzyl ether is favored increasing the reaction time (see Table 3.7). The performances of this catalytic system were consistent with those reported in literature in terms of conversion using palladium intercalated bentonite catalyst (95% after 5 h at 100°C) but in this last case increasing the temperature from 50 to 100°C has a detrimental effect on the selectivity[8] . For all the experiments performed, carbon balance based on the carbon content in the

unconverted aldehydes and in the hydrogenation products is systematically calculated (>95%). Finally, the catalyst presents also a good recyclability maintaining good conversion(>90%) and selectivity (>99%) after 3 cycles of use and resulting in a drop of the catalytic performance only at fourth cycle (70%).

Table 3.7 Effect of time on selectivity using Pd/C at 120°C.

Catalyst	Time (h)	Conversion %	Benzyl alcohol %	Benzyl ether %
Pd/C	0,25	33	88	12
	0,5	57	86	14
	1	70	80	20
	3	87	15	85
	5	92	13	87

Reaction conditions: 0.025g catalyst, 2.5 mL benzaldehyde, 10 mL diethyl ether, 8 bar H_2.

In order to assess the effect of metal loading on the catalytic activity a Pd/Mayenite catalyst with a metal loading of 10% was also prepared. Metal content was chosen equal to that used in commercial Pd/C in order to have a more tight comparability. Pd/Mayenite 10% wt shows a BET surface of 2.1 m^2/g sensibly lower than that observed for 1% Pd/Mayenite (16.9 m^2/g) and, as evidenced by SEM analysis, (see Figure 3.21) a not uniform distribution of the metal on

mayenite resulting in the formation of aggregates.

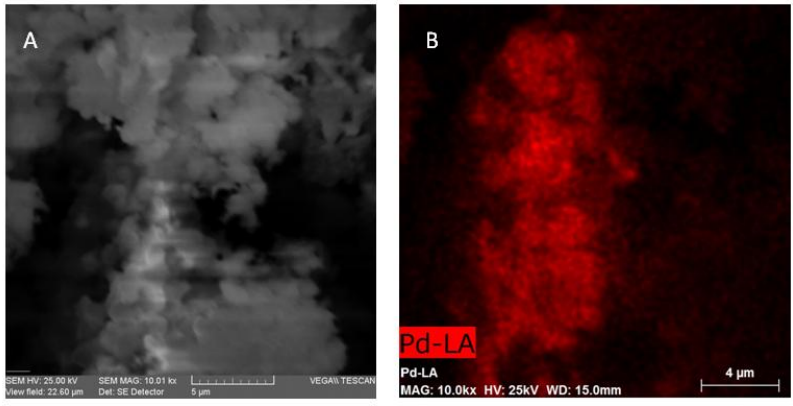

Figure 3.21 SEM image (A) and relative map of Pd distribution of sample with Pd concentration of 10% (B).

As expected on the basis of these morphological observation, the performances of Pd/Mayenite 10% wt catalyst, under the same reaction conditions, drop down (only 10% after 5h) compared to the same catalytic system with a metal loading of 1 % (91% after 5h).

In order to tests the selectivity in a multifunctional molecule, palladium loaded mayenite (1% wt) was also employed in the hydrogenation of cinnamaldehyde. Hydrogenations were carried out using both Pd/C and Pd/Mayenite catalysts using the optimized conditions, in terms of conversion, for benzaldehyde. (t= 5 h; T=120°C; P (H_2)= 8 bar; 10 mL of Et_2O as solvent). As reported in literature, hydrogenation of cinnamaldehyde leads to different products depending on the

active metal, solvent and promoter[9]. The possible product originating by cinnamaldehyde hydrogenation are reported in Scheme 1.

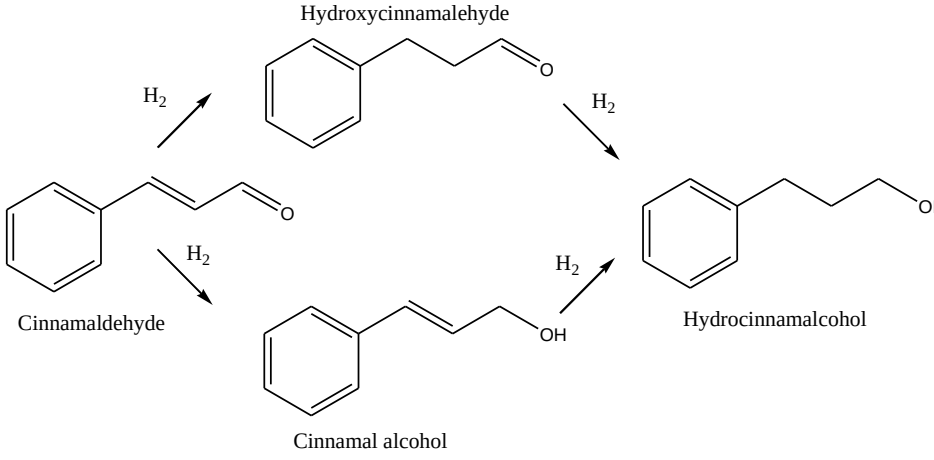

Scheme 1. Selective hydrogenation of cinnamaldehyde.

Under these conditions, on one hand the Pd/C catalyst converts quantitatively the substrate giving the hydrocinnamalcohol as main product (65%) and hydroxycinnamaldehyde (35%). On the other hand using Pd/Mayenite the conversion is also quantitative with 83% of hydroxycinnamaldehyde and 17% of hydrocinnamalcohol showing an higher selectivity toward the reduction of double bond respect to the aldehydic function. Results confirm the wide applicability of the palladium loaded mayenite as hydrogenation catalyst to different aldehydes with excellent performance.

3.3.5 Conclusions

In this thesis, mayenite substrate was used for the first time, as active catalyst support for palladium and the resulting catalyst was fully characterized. Pd/Mayenite catalyst was employed in the catalytic reduction of benzaldheyde showing high performances in terms of conversion and selectivity compared to commercial Pd/C catalyst. In particular, mayenite substrate shows to be a robust support also at high temperatures (120 °C) inhibiting byproduct formation and preserving an high selectivity in the benzyl alcohol production. A preliminary study conducted on the cinnamaldehyde hydrogenation reaction confirms the applicability of Pd loaded mayenite as an effective catalyst to a wide range of substrates.

References

(1)M. Cherian et al., *Appl. Catal. A: Gen.* **2002**,233,21-33
(2)Z. A. Alothman, *Materials* **2012**,5,2874-2902
(3)K. Hayashi et al., *J.Am.Chem.Soc.***2002**,124,738-739
(4)L. Wang et al., *Carbon* **2012**,50,3134-3140
(5)T. Yoshizumi et al., *J. Phys. Chem. C* **2012**,116,8747-8752
(6)K. Hayashi et al., *Nature*,**2012**,419,462-465
(7)O. B. Belskaya et al., *Theor. Exp. Chem.* **2013**,48,381-385
(8)D. Divakar et al., *Catal. Lett.* **2008**,125,277-282
(9)X. Yang et al., *J. Catal.* **2012**,291,36-43

APPENDIX A

University of Salerno

Department of Chemistry and Biology

Ph.D Course in Chemistry
(XIII Cycle)

PROJECT "DOTTORATI IN AZIENDA"

In collaboration with Cle.Pr.In srl

Academic year 2013-2014

Preface

During the Ph.D course I spent some months in Cle.Pr.In srl in Sessa Aurunca (CE), Italy. Cle.Pr.In srl is an important industry, leader in the production of detergents for professional use.

This collaboration is financed by Regione Campania (FESR POR-Campania 2007-2013).

This appendix presents the main results of industrial research relevant for economic and applicative scopes for Cle.Pr.In srl.

It consists in the study of an antibacterial chemical formulation for household waste management.

At the moment product developed during my Ph.D project are commercially available, and a new production system was initiated at Cle.Pr.In. srl.

Product on market (Antibacterial formulation on cellulose based filter).

I) Antibacterial chemical formulation for the household waste management

Abstract

The novelty of this work is related to the combination of different antimicrobial components with different volatility studying the antimicrobial activity of the gas phase. These components have been previously singularly tested as antimicrobial agents in liquid phase at direct contact with the microbes, the novelty of this study is linked to their use as mixture to sanitize small environments where the vapour phase can diffuse avoiding the microbes growth. This study proposes a new bactericidal mixture able to inhibit bacterial proliferation and useful in the management of waste during the storage in the apartments.

Introduction

A wide range of events have served to underline the need for renewed action in relation to infectious disease. As a significant part of this there is awareness of the importance of placing prevention through hygiene at the core of national strategies aimed at infection control[(1)]. Of significance is also a growing of the strategic importance of the domestic setting in the chain of infection transmission through the community[(2)]. Encouraging the concept of the home as a setting in which the whole range of activities occur, including food hygiene, personal hygiene, hygiene related to medical care and first management of domestic waste provides the opportunity for a rational approach to home hygiene based on risk assessment.

These indications induce to improve the current practice and promote an improved hygiene in the domestic setting as a strategy to reduce infectious disease.

Surely greater assistance to the handling of household waste may provide better prevention of the spread of micro-organisms in the house, even more so in recent years in which the culture of waste separation spreads in almost all countries. This practice requires that waste persists for longer times in the apartments favouring the spread of unpleasant odour due to the proliferation of microorganisms able to feed household

waste. Our research fits in this scenario, and aims to identify simple and especially not harmful strategies for the prevention of the spread of odours and proliferation of microbes contained in the waste.

Our attention is focused on antimicrobial herbal drugs which may be employed to extract the essential oils (EO) largely employed for their antibacterial, antifungal and insecticidal properties[3]. Among them, a valid example is the oxygenated monoterpene detected in mandarin EO, limonene oxide known to be active against a wide spectrum of pathogenic fungi and bacteria tested[4]. Moreover the antimicrobial activity of essential oils (EOs) of cinnamon has been considered on Gram-positive, Gram-negative bacteria and fungi[5-8]. These substances are generally regarded as safe and are used as flavouring agents in the food[9]. In addition to exhibiting antibacterial activity, cinnamaldehyde also inhibits mold growth and mycotoxin[10]. It is also used as an ingredient in fine fragrances, shampoos, toilet soaps and other non-cosmetic products such as household cleaners and detergents[11].

Cinnamaldehyde and many other components extracted from other EOs have been registered by the European Commission and are considered riskless to the health of customers[3]. Therefore, we considered them interesting and useful to

improve domestic hygiene.

Our aim was to combine the antimicrobial effects of cinnamaldehyde with limonene and isopropanol in order to increase their antimicrobial potential and to decrease the microbial resistance. The purpose of this study was to take advantage from their high volatility and nice smell to destroy the stink and decrease the microbial charge of domestic waste.

Materials and methods

Reagents

Trans-cinnamaldehyde, 2-propanol were provided by Sigma-Aldrich (Missouri, USA). Propylene glycol was provided by Carlo Erba Reagents s.r.l. (France). Orange terpenes and Eucaliptus glob. oil were supplied by L.R. Composizioni Profumanti s.r.l. (Bologna, Italy). Moreover, the Neem oil-tonic was supplied as a mix of enriched Neem oil (70%), emulsifier (sapindus trifoliatus water extracted with soya lecithin, 10%), UV stabilizer (epoxidised soybean oil, 10%), anti oxidant (absorbic acid with grape seed oil, 10%) by Parker enterprises (Chennai, India). The antimicrobial two-phase mixture tested in this paper has the reagent composition showed in table A1.

Table A1. Reagent composition of antimicrobial mixture.

Compound	Mix % v/v
2-propanol	32,5
Propylen glycol	21
Neem-oil tonic	5
Trans-cinnamaldehyde	10
Orange terpenes	2
Eucaliptos oil	1,5
water	28

Microorganisms and media

Bacterial strains *Escherichia coli* JM109 (Promega Cat. n. 9451), *Staphylococcus aureus*, the yeast *Debaryomyces hansenii* and the mold *Penicillium citrinum* were obtained from the collection deposited in the A. Proto's laboratory. They were deep frozen for storage and they were grown on LB agar. Colonies from this agar were grown in LB broth (Oxoid) at 37°C overnight to 10^9 colony forming units (cfu)/ml, the black molds have been crumbled by pottering and then were grown on LB agar and counted. LB broth served as a test medium for the antimicrobial activity of the bactericidal mixture.

Minimal inhibitory concentration (MICs) of antimicrobial mixture

The MIC is determined as the lowest concentration of the antimicrobial agent that will be able to inhibit the visible growth of a microorganism. MIC of mixture was determined after 24 h incubation of *Escherichia coli* 5 x 10^6 cfu/ml in LB broth with increasing concentration of antimicrobial mixture (e.g.: 0.4 µl/ml, 0.95 µl/ml, 1.9 µl/ml, 3.8 µl/ml, 7.6 µl/ml, 15.2 µl/ml, 30.4 µl/ml). The minimum bactericidal concentration (MBC) was identified by determining the lowest concentration of bactericidal mixture that reduces the viability of the initial inoculum up to 99.9%.

Antimicrobial activity of the mixture's vapour phase with time

To evaluate the capability of gas emitted by the mixture to kill the microbial cells, 2 ml of mixture, under constant agitation, was spread on a Whatman paper sheet (10 x 4 cm) and this sheet was closed in a glass beaker (capacity: 800 ml) covered with an aluminium paper. In every beaker LB agar plates were inserted. On each plate different diluition of a known quantity of one among four different analyzed microorganisms: *Staphylococcus aureus, Escherichia coli, Debaryomyces hansenii* or *Penicillium citrinum,* was spread. Each plate was

left one week in the beaker with the antimicrobial mixture (experimental groups) or without antimicrobial mixture (control groups) at room temperature and at the end the number of CFU formed was counted. Every week, for four consecutive weeks, the plate, with approximately the same bacterial charge, was replaced to observe the efficiency of antimicrobial vapour phase with time.

Chemical evaluation of the mixture's vapour phase during the weeks of testing

To estimate the amount of gas emitted by the mix spotted on the sheet during the weeks, 100µL of gas taken from the top of the beaker, with a gas-tight Hamilton syringe, was analyzed using a Agilent model 7890A gas chromatograph equipped with a flame ionization detection (FID) system, each week (for four successive weeks). The GC separation column was a 60m x 0.25mm i.d HP-5MS fused silica capillary column (Agilent Technologies). The carrier gas was helium at 1.0mLmin^{-1}; injector and detector port were respectively, 210°C and 260°C; oven temperature 35°C (hold for 2 min), rate 1°Cmin^{-1} to 60°C (hold 2 min), rate 5°Cmin^{-1} to 200°C (hold 5 min).

Results and discussion

The mixture was tested for its antimicrobial activity against the Gram negative bacteria *Escherichia coli* and pathogen Gram positive *Staphylococcus aureus* and the fungi *Debaryomyces hansenii* and the mold *Penicillium citrinum*. The tested microorganism are known for their capability to proliferate in house waste material. They are abundantly diffused in vegetables, fruits, undercooked beef, unpasteurized milk and juice, in cellulose-rich materials, for all these reasons they are considered ideal candidate for our study[12-15]. In particular, the antimicrobial capability of the vapour phase of the mixture on the microorganisms' growth was tested.

The mixture was spread on a Whatman paper sheet (10 x 4 cm) and this was inserted in a glass beaker containing LB agar plates on which different dilutions of a known title of the analyzed microorganisms (about 10^6 cfu/ml *Escherichia coli,* 10^6 cfu/ml *Staphylococcus aureus,* 10^5 cfu/ml *Debaryomyces hansenii* or 10^5 cfu/ml *Penicillium citrinum*) were spread. Each experimental setting was completed by a series of control groups composed by plates with a countable number of colonies (dilution 10^{-4}) of bacteria or fungal cells incubated in the beaker without antimicrobial mixture.

The vapour phase of antimicrobial mixture showed to be able to avoid bacterial and fungal growth for at least three weeks, during which a complete inactivation of all tested microorganisms was registered (see table A2). On the contrary, it resulted not to be able to control the bacterial proliferation during the fourth week. In fact, the remaining vapour phase allowed the growth of both *E. coli* and *S. aureus*. However the motile *E. coli* showed a net phenomenon of chemotaxis, as the bacteria developed only in the opposite side with respect to that where the sheet soaked by antimicrobial mixture was placed.. This would indicate that at the fourth week a toxic effect on the bacteria still persists near the sheet. Nevertheless, after four weeks, the remaining vapour phase was efficient to control the fungi proliferation, probably because they present a greater susceptibility respect to bacteria to vapour phase components.

Table A2. Antimicrobial effect of mixture's vapour phase during the weeks. The number of CFU is considered n.c. when they were not countable for the presence of a high density of colonies.

Experimental group	**Microrganisms**	**CFU/ml after 1 week**	**CFU/ml after 2 weeks**	**CFU/ml after 3 weeks**	**CFU/ml after 4 weeks**
CNT +	*Escherichia coli*	86×10^5	28×10^6	54×10^6	35×10^6
Antimicrobial Mix	*Escherichia coli*	0	0	0	n.c.
CNT +	*Debaryomyces hansenii*	14×10^5	17×10^5	10×10^5	13×10^5
Antimicrobial Mix	*Debaryomyces hansenii*	0	0	0	0
CNT +	*Penicillium citrinum*	64×10^4	66×10^4	64×10^4	60×10^4
Antimicrobial Mix	*Penicillium citrinum*	0	0	0	0
CNT +	*Staphylococcus aureus*	21×10^6	13×10^6	17×10^6	36×10^6
Antimicrobial Mix	*Staphylococcus aureus*	0	0	0	n.c.

The aim of this study was to formulate a product that could be used to aid in solving the problem of household waste management. For this reason we chose harmless and natural components that are known for their antimicrobial properties, such as Neem oil, cinnamaldehyde and orange terpenes (i.e. Limonene) natural antimicrobial compounds that have already been tested on different species of microorganisms[4,5,16,17].

Another important characteristic for this formulation was the time extent. Our aim was to create a product easy to use, efficacious and durable. To be sure about its duration and efficacy from the first hours of treatment up to several weeks we chose for this mixture microbicidal components with different volatility, i.e. 2-propanol and limonene with high vapour tension and cinnamaldehyde with low vapour tension.

A representative chromatogram of the emitted mixture gas phase is reported in Figure 1. It shows a good separation between the analyzed compounds. As reported in figure 2, 2-propanol and limonene were predominant for the first two measures (time = 0 and 24h) while trans-cinnamaldehyde was released from the mixture in correspondence of 2-propanol and limonene removal due to their different vapour density. Propylen glycol, used as dispersing agent, showed a lower concentration compared to the other components of the mixture. The trans-cinnamaldehyde concentration showed a

slow increment until 24 hours while from the first week to the third week it was the predominant component in the gas phase.

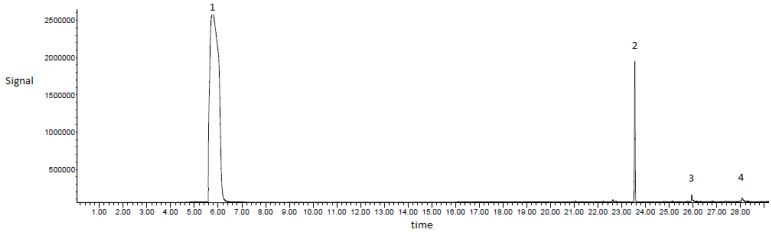

Figure A1. Chromatogram of the mixture(2-propanol(1), limonene(2), propylen glycol(3) and trans-cinnamaldehyde(4)) obtained under working conditions.

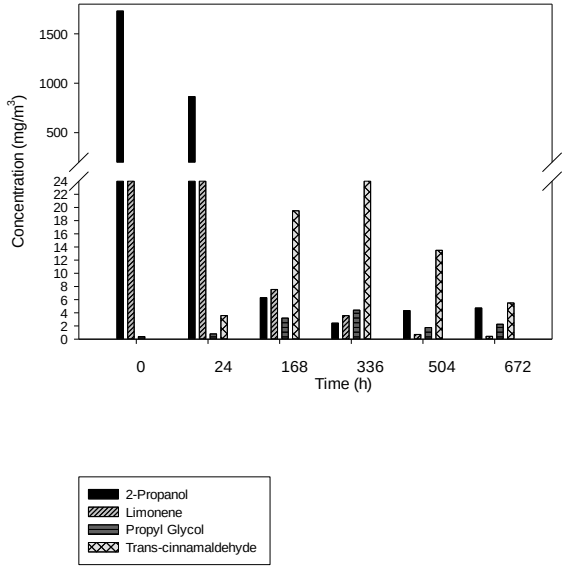

Figure A2. Variation of composition of vapour phase of antimicrobial mixture during the weeks.

The experimental data testify the duration of mixture vapours (figure A2) and their microbicidal efficacy (table A2). Our results show that the antimicrobial effect of the mix during the first 24 hours is most probably due to the combined functions of 2-propanol and limonene. These two components are largely employed as antimicrobial agents for their efficacy against both bacteria and fungi, but probably their higher volatility has conditioned their previous use as disinfectants able to act at direct contact with microorganism and in some cases entrapped in gel matrix to extent their half life[4,18].

During the remaining twenty-seven days of our tests, the antimicrobial effect was mediated by the cinnamaldehyde. In the last week (fourth), the remaining vapour phase of cinnamaldehyde had not a sufficient effect to avoid the growth of bacteria (Gram + and Gram -), whereas it was sufficient to control the fungi growth, probably because they are more sensible to cinnamaldehyde, as also suggested by previous studies[5]. Previous works, in fact, testify that the percentage of inhibition induced by the same concentration of cinnamaldehyde vapours is higher for some fungi and mold species in respect to that necessary for Gram + and Gram – bacteria. Following the tests to measure the concentration of each component of the mix into the gas phase and measuring the antimicrobial efficacy of this vapour phase, we tested the

potentiality of this mixture to sanify small environment such as waste bucket. This kind of application is new and could have a high commercial potentiality because the single components of this bactericidal mix have been known and used, until now, as efficient microbicidal agent in direct contact with the surface[19], skin[18], food[17] but their vapour phase is only poorly considered as disinfectant agent[5].

Moreover we tested the efficacy of the mixture in liquid phase on *Escherichia coli*.

The results of MIC and MBC tests are represented in Figure A3. The concentration of antimicrobial mixture able to inhibit a visible growth of *Escherichia coli* is 1.9 µl/ml. In this condition, the number of inoculated cells did not significantly change after 24 h. On the other side, the mixture concentration able to eliminate the 99.9% of bacterial cells was in the range 3.8 - 7.6 µl/ml.

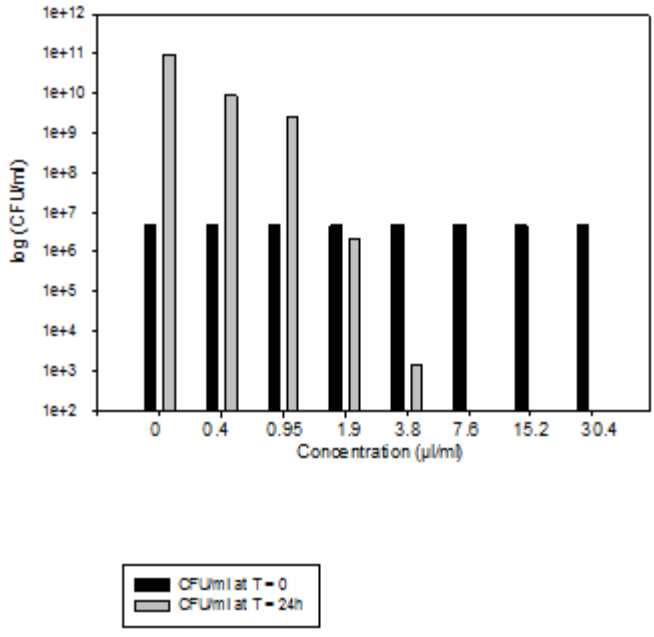

Figure A3. Effect of antimicrobial mixture in liquid phase on *Escherichia coli* as a function of concentration.

These results show an improvement of antimicrobial efficacy of each mixture components. The presence of a synergic action of several antimicrobial agents improves the microbicide efficacy requiring a lower dose of each component respect to what is reported in previous studies[21]. The MIC of cinnamaldehyde against *E. coli* has been reported to be 400 mg/L by Pei and coworkers [21], whereas in our

conditions, the synergic effect of several antimicrobial agents made 199 mg/L of cinnamaldehyde sufficient. A similar result was obtained for limonene. The quantity estimated for MIC against *E. coli* was 1.50 mg/ml, whereas in our case 0.032 mg/ml were sufficient to inhibit the bacteria growth.

Conclusions

In conclusion, the synergic effect of some known antimicrobial agents gives rise to a product with a pleasant odor, good microbicidal performances and long lasting effect. The antimicrobial activity of the new microbicide mixture was evaluated over a range of concentration in two type of tests (liquid and vapour diffusion) against both bacteria and fungi. Bacteria proliferation was prevented for the first three weeks of the experiment whereas fungi growth was inhibited up to 4 weeks due to the inhibition effect of cinnamaldehyde vapours. Chemical analysis was performed in order to better identify the component in the vapour mix for the entire duration of the experiment and it showed that trans-cinnamaldehyde was the major component in the last part of the experiment.

From the results here reported it can be asserted that this chemical formulation has the potential to be applied in domestic waste treatment favouring home hygiene and avoiding the smell diffusion.

References

(1)S.F. Bloomfield, *Int. J. Envir. Health.* **2003**,206,1-8
(2)S. Settar et al., *Am. J. Infect. Contr.* **1999**,27,4-21
(3)S. Burt, *J. Food. Microb.* **2004**,94,223-253
(4)K. Aggarwal et al., *Flav. Fragr. J.* **2002**,17,59-63
(5) P. Lopez et al., *J. Agric. Food. Chem.***2005**,53,6939-6946
(6)S. Ravishankar et al.,*J. Food. Prot.* **2010**,73,234-240
(7)F. Donsi et al., *Food. Sci. Tech.* **2011**,44,1908-1914
(8)P. Dahiya et al., *J. Pharm. Sci.* **2012**,74,443-450
(9)L.S.M. Ooi et al., *Am. J. Chin. Med.* **2006**,34,511-522
(10)C. Bilbao-Sainz et al., *J. Am.Oil. Chem. Soc.* **2013**,90,233-241
(11)J. Cocchiara et al., *J. Chem. Toxicol.* **2005**,43,867-923
(12)P. Martorell et al., *J. Food. Microb.* **2005**, 101,293-302
(13)W.J. Meggs, *Toxicol. Ind. Health* **2009**,25,571-576
(14)W. Vanderhaeghen et al.,*Epidemiol. Infe.* **2010**,138,606-625
(15)N. Aboutaleb et al., *Curr. Opin. Gastroenterol.* **2014**,30,106-115
(16)M.D.M. Hoque et al., *Food. Pathog. Dis.* **2007**,4,481-488
(17)W. Do et al., *J. Food. Sci.* **2009**,74,372-378
(18)M.H. Kirshner et al., *Langen. Arch. Surg.* **2009**,394,151-15
(19)G. McDonnell et al., *Clin. Microbiol. Rev.* **1999**,12,147-179
(20)R. Pei et al., *J. Food Sci.* **2009**,74,379-383

Acknowledgements

Al termine di questo entusiasmante percorso sento il dovere ed ho il piacere di ringraziare chi lo ha condiviso con me.
Prima di tutto, il Professore Proto per avermi permesso di crescere liberamente sotto la sua guida intelligente, sia dal punto di vista scientifico che umano. Porterò sempre con me la gioia con la quale ho affrontato questi anni grazie a lui. Grazie per le responsabilità affidatemi e per la fiducia che avete riposto in me.
Grazie al Dr. Federico Rossi con il quale ho avuto l'onore di collaborare, per la grande umanità e la disponibilità ad aiutarmi nel migliorare, sempre.
Grazie alla Professoressa Motta per il costante aiuto e confronto.
Desidero ringraziare il Dr. Carmine Capacchione per avermi motivato nel migliorare la mia ricerca.
Ringrazio il Prof. Venditto per aver migliorato il mio percorso di dottorato e l'elaborato di tesi attraverso un confronto schietto volto a criticare in maniera costruttiva e propositiva.
Grazie al Prof. Guerra ed al Prof. Oliva per la sagace guida e disponibilità.
Grazie alla Dr.ssa Genga e ad al Dr. Scicali per aver condiviso insieme progetti e soddisfazioni.

Ringrazio la Dr.ssa Zarrella, per la proficua collaborazione ed il piacere quotidiano nel lavorare insieme.
Ringrazio la Cleprin srl nella persona di Antonio Picascia per aver arricchito il mio percorso di dottorato guardando la ricerca scientifica anche da un punto di vista industriale e in termini applicativi, per aver accolto le mie proposte, per aver suggeriti nuovi orizzonti e per l'entusiasmo contagiante.
Grazie ai miei compagni del laboratorio 8, Maria, Marianna e Milo, grazie ai quali in questi anni ho trascorso giornate in famiglia.
In particolare, ringrazio di cuore il mio amico Milo con il quale da anni vivo a stretto contatto per avermi sempre aiutato in maniera disinteressata, con sincerità e amicizia vera.
Grazie a tutti i ragazzi e le ragazze che hanno svolto la tesi nel nostro laboratorio, ciascuno di voi ha arricchito il mio percorso: Adriano e Concetta augurandovi sempre il meglio per il futuro, Francesca per la smisurata bontà, Maria, Emanuele, Salvatore, Stefano, Astrid, Irene, Raffaella, Rosa.
Grazie agli amici di sempre, Gerardo, Alessandra, Maurizio, Alessia, con i quali anni fa intrapresi il percorso universitario e con i quali ho avuto il piacere di condividere anche il dottorato.
Ringrazio Patrizia, Ivano, Patrizia e il signor Mormile per l'arte del saper fare sapientemente condivisa.

Grazie a chi ha camminato al mio fianco con sincerità a chi gioisce con me in questo giorno, ai miei amici di sempre , alla mia famiglia e a chi non c'è più.